View Article Online
DOI: 10.1039/C8PP00492G

UVR8-dependent reporters reveal spatial characteristics of signal spreading in plant tissues

Lucas Vanhaelewyn[1], Péter Bernula[2,3], Dominique Van Der Straeten[1], Filip Vandenbussche[1], András Viczián[2*]

1. Laboratory of Functional Plant Biology, Department of Biology, Faculty of Sciences, Ghent University, KL Ledeganckstraat 35, B-9000 Gent, Belgium
2. Institute of Plant Biology, Biological Research Centre, Temesvári krt. 62, H-6726 Szeged, Hungary
3. Doctoral School in Biology, Faculty of Science and Informatics, University of Szeged, Szeged, H-6726, Hungary.

*Corresponding author:

Tel: 00-36-62-599717

Fax: 00-36-62-433434

E-mail: viczian.andras@brc.mta.hu

Abstract

The UV RESISTANCE LOCUS 8 (UVR8) photoreceptor controls UV-B mediated photomorphogenesis in Arabidopsis. The aim of this work is to collect and characterize different molecular reporters of photomorphogenic UV-B responses. Browsing available transcriptome databases, we identified sets of genes responding specifically to this radiation and are controlled by pathways initiated from the UVR8 photoreceptor. We tested the transcriptional changes of

View Article Online
DOI: 10.1039/C8PP00492G

several reporters and found that they are regulated differently in different parts of the plant. Our experimental system led us to conclude that the examined genes are not controlled by light piping of UV-B from the shoot to the root or signalling molecules which may travel between different parts of the plant body but by local UVR8 signalling. The initiation of these universal signalling steps can be the induction of ELONGATED HYPOCOTYL 5 (HY5) and its homologue, HYH transcription factors. We found that their transcript and protein accumulation strictly depends on UVR8 and happens in a tissue autonomous manner. Whereas HY5 accumulation correlates well with the UVR8 signal across cell layers, the induction of flavonoids depends on both UVR8 signal and a yet to be identified tissue-dependent or developmental determinant.

Introduction

Ultraviolet B (UV-B: 280-315 nm) radiation is an integral part of sunshine reaching plants that depend on solar light as energy source. Apart from damaging organic macromolecules[1-3], UV-B also acts as a physiological signal contributing to normal plant development. To monitor this environmental trait, plants have developed the UV-B-specific photoreceptor, UV RESISTANCE LOCUS 8 (UVR8). Since its discovery[4-7], this photoreceptor has been associated with a diverse array of responses, including flavonoid biosynthesis, inhibition of hypocotyl extension, leaf expansion, endoreduplication, stomatal density and closure, entrainment of the circadian clock, tolerance to *Botrytis*, response to osmotic stress, phototropism, leaf epinasty, and inhibition of thermomorphogenesis (for a summarizing review see: Jenkins, 2017[8]).

Upon UV-B exposure, tryptophan amino acids of the UVR8 dimers absorb the radiation. Some tryptophans at special positions are closely associated with crucial salt-bridge amino acids which maintain the dimer state[7,9,10]. According to our current knowledge, the neutralization of these salt bridges by the action of the chromophore tryptophans leads to the monomerization of the photoreceptor[11-15]. This monomerization process causes conformational changes and therefore frees previously inaccessible regions which then allow UVR8 to interact with proteins, like CONSTITUTIVELY PHOTOMORPHOGENIC 1 (COP1) and starting a signalling cascade[7,16-18]. COP1 in complex with SUPPRESSOR OF PHYA-105 (SPA) proteins act as a repressor of photomorphogenesis by targeting positive regulators of light responses such as ELONGATED HYPOCOTYL 5 (HY5) for degradation via ubiquitination[19-22]. UV-B-induced binding of UVR8 monomers with COP1 reduces the targeted proteolysis of HY5 leading to its stabilization[4,23]. HY5 positively regulates its own transcription and therefore promotes additional HY5 accumulation[24]

View Article Online
DOI: 10.1039/C8PP00492G

which enables transcription of a wide range of UVR8 target genes, making HY5 a key regulator of the UVR8-driven signalling. UVR8 monomers can also interact directly with WRKY DNA-BINDING PROTEIN 36 (WRKY36) removing this transcriptional inhibitor from the *HY5* promoter thus leading to enhanced *HY5* transcription under UV-B irradiation[25].

The UV-B induction of photoprotective pigment accumulation has been used as hallmark of UV-B sensitivity. Under photomorphogenic doses of UV-B irradiation UVR8 signalling has a crucial role in this response as the pathway is necessary to turn on flavonoid biosynthesis[5]. It is generally assumed that flavonoids accumulate in the epidermis to protect plants from potentially damaging UV-B radiation. UV-B induces *PHENYLALANINE AMMONIA LYASE* (*PAL*), *CHALCONE SYNTHASE* (*CHS*), *CHALCONE FLAVANONE ISOMERASE* (*CHI*), *FLAVONOL SYNTHASE* (*FLS*), *FLAVANONE 3-HYDROXYLASE* (*F3H*) and both kaempferol and quercetin derivatives accumulate upon UV-B exposure in Arabidopsis seedlings[26]. Besides the UVR8-independent light and stress pathways, at least *CHS*, *CHI* and *FLS* were shown to be regulated by HY5[5,27-30].

Gene regulation upon UV-B radiation has been studied on multiple occasions, in different laboratories, using different methods, various species and/or mutants, different light sources, different time points for sampling and different target tissues. Consequently, the outcome of these studies varies widely. Nevertheless, apart from the above mentioned flavonoid biosynthesis genes, some genes have been identified and used as reporters for UVR8 signalling: *HY5, CHS, HYH, ELIP1, CRYD*, *GPX7, SIG5, PHR1, WAKL8* with the first two as most implemented examples[4,6,24,28,31-34]. At this point we do not know whether these genes are universally applicable as markers for UV-B or UVR8 signalling thus a more comprehensive approach to categorize the ensemble of marker genes would be a solid basis for further studies.

Studying optical characteristics of plant tissues[35] has begun a revival[36,37] in recent years. In addition to this, several studies have shown that the perception of light cues lead to tissue specific and inter-tissue signalling, including various molecular responses and complex phenotypic traits[38-45]. A recent study showed that white light, after reaching shoots can travel through the tissues by an effect called light piping, and can generate photomorphogenic responses in the roots which are not directly exposed to light[46]. Furthermore, within the roots, red light appears to travel more efficiently than blue light to entrain the circadian clock in distal unexposed tissues[47]. These studies indicate that this physical phenomenon can substantially contribute to rapid signal spreading throughout the plant body. Currently, no data have been reported on light piping of UV-B, although it was already demonstrated that a yet unidentified signal caused by UV-B treatments spreads quite fast within the plant tissues from the irradiated organs to the shaded ones in maize[48]

View Article Online
DOI: 10.1039/C8PP00492G

Here we evaluate the means of detecting differences in UVR8 signalling based on currently available scientific resources. Genes with reporter potential are listed and the potential of flavonoid accumulation as the phenotypic manifestation of UVR8 signalling is monitored using transgenic lines expressing UVR8 only in certain tissues. Furthermore, we set up an experimental system and selected reporter genes to study the possibility of light piping and transfer of UVR8 signalling components under UV-B irradiation in Arabidopsis.

Materials and methods

Plant materials and molecular cloning. *Arabidopsis thaliana* wild type (Columbia) and *uvr8-6* mutant[4] were used for the transcript analysis. These backgrounds expressing *pHY5:HY5-GFP*[44] or *pHYH:HYH-GFP* transgenes were used to follow HY5-GFP and HYH-GFP protein accumulation by western blot and the spatial distribution by confocal laser scanning microscopy. *pML1:YFP-UVR8/uvr8-6, pUVR8:YFP-UVR8/uvr8-6, pCAB3:YFP-UVR8/uvr8-6 and pSUC2:YFP-UVR8/uvr8-6* transgenic plants were described by Bernula et al, 2017[44].

The *pHYH* promoter (*Hind*III-*Bam*HI) and the coding region of *HYH* (*Bam*HI-*Sma*I) were inserted into the *pHY5:HY5-GFP pPCV812* binary vector[42] resulting in *pHYH:HYH-GFP pPCVB* what was used to transform Col and *uvr8-6* backgrounds. The cloned *pC1* promoter (AT1G09750) and the *pSCR* promoter (AT3G54220) (kind gift from Miguel Blázquez (Valencia, Spain)) were cloned together with the YFP-UVR8 coding sequence into the pH7m24GW binary vector[49] using the Gateway™ cloning method according to the manufacturer's instruction (Invitrogen). The resulted *pH7m24GW-pC1:YFP-UVR8* and *pH7m24GW-pSCR:YFP-UVR8* constructs were used to transform *uvr8-6* mutants. Plant transformation, methodology and principles of transgenic line selection are described in detail by Kirchenbauer *et al.,* 2016[42]. The *p35S:GFP*/Col line was described earlier[50].

***In situ* flavonol staining.** Arabidopsis seedlings were grown on horizontal half strength Murashige and Skoog (Duchefa) medium with 1% sucrose and 0.8% plant tissue culture agar (LABM) in white light (52 µmol m^{-2} s^{-1} of photosynthetically active radiation light (PAR)) for 2 days and subsequently exposed to 1 µmol m^{-2} s^{-1} 311 nm adaxial UV-B (narrowband, Philips TL01) for 3 days. Negative controls, having no UV-B treatment were covered with a filter blocking UV-B (Jürgen Rachow). The seedlings were directly mounted on microscope slides with an aqueous solution of diphenylboric acid-2-aminoethyl ester (DPBA) comprising 0.25% (w/v) DPBA and 0.00375% (v/v) Triton X-100 and incubated for 5 minutes prior to visualization. The samples were

View Article Online
DOI: 10.1039/C8PP00492G

analysed by confocal laser scanning microscopy (Nikon, EZ C1). DPBA-stained flavonoids were visualized by 405 nm excitation light, while YFP was visualized using 488 nm excitation light. DPBA and HY5-YFP (seedlings mounted in water) were monitored in distinct plants. Emission was detected in the 515-530 nm range.

Meta analysis of differentially regulated gene sets. Published gene lists were combined based on Venny intersections[51]. Output lists were generated using the read out of Venny intersections. For the first list of repeatedly UV-B upregulated genes, the gene list for 1 and 6h of Favory *et al.,* 2009[4] were combined, while the Ler and Col list of Oravecz *et al.,* 2006[52] were kept separated. To these three lists, the list by Brown and Jenkins, 2008[28] was added (Supplementary Fig. 1) and genes appearing in the intersection of at least three of the four datasets were kept as candidate UV-B marker genes (yielding the list of 264 genes). Furthermore, the dataset of Vandenbussche *et al.,* 2018[53] was kept as it was, the datasets of Wan *et al.,* 2018[54] of UV-B regulated genes at 0.5 and 2h were combined.

Total RNA analysis and determination of transcript level. Columbia wild type and *uvr8-6* mutant seeds were surface sterilized and kept in the dark at 4 ºC for 72 h. The seedlings were grown vertically on half-strength Murashige-Skoog medium (Sigma-Aldrich) containing 1% sucrose and 1% agar at 22 ºC under 12h dark/ 12h light regime for 11 days. Before sample collection, the seedlings were irradiated with white light (PHILIPS TL-D 18W/33-640 tubes, 10 μmol m^{-2} s^{-1}) supplemented with photomorphogenic UV-B (PHILIPS ULTRAVIOLET-B TL20W/01RS tubes, 1.5 μmol m^{-2} s^{-1}) for 120 min. The emitted radiation was narrowed by transmission cut-off filters of the WG series (Schott). The UV-B-treated seedlings (+UV-B) were covered with WG305 filter with half-maximal transmission at 305 nm as described previously[34] whereas the non-UV-B irradiated control seedlings were covered with WG385 filter with half-maximal transmission at 385 nm (-UV-B). The shoots (hypocotyl and cotyledons) and roots were dissected, collected separately and snap frozen in liquid nitrogen. Alternatively, plants were irradiated with UV-B while their roots were covered with aluminium foil whereas the shoots not. Furthermore, plant samples which had the roots and shoots separated during the irradiation treatment were also collected. Supplementary Fig. 2 depicts the experimental setup. Total plant RNA was isolated using the Nucleospin Plant II Maxi kit (Macherey-Nagel) according to the manufacturer's instruction. The reverse transcription was made using the RevertAid First Strand cDNA synthesis Kit (Thermoscientific) and the qRT-PCR reaction using the qPCRBIO Sygreen Mix (PCR Biosystems) following the instruction of the manufacturers. Supplementary Table 1.

View Article Online
DOI: 10.1039/C8PP00492G

shows the sequence of the used oligonucleotides for the qRT-PCR assays. The presented graphs show mRNA levels relative to the constitutively expressed *TUBULIN2/3* mRNA transcript[41].

Plant protein extraction and western blot analysis. Columbia wild type and *uvr8-6* mutant lines expressing *pHY5:HY5-GFP* or *pHYH:HYH-GFP* transgenes were grown as for transcript analysis. 10-day-old seedlings were irradiated with UV-B mixed with white light as described in the previous paragraph for 20h. All root-shoot separation, irradiation treatments and sample collection is described above. For the protein extraction plant materials was homogenized in boiling SDS sample buffer [65 mM Tris–HCl (pH 6.8), 7% SDS, 4 M urea, 15% glycerol, 6% ß-mercaptoethanol, 0.05% bromophenol blue] and was incubated at 95 °C for 2 min. The plant homogenate was cleared by centrifugation (20 min at 20,000 *g* at 25 °C) and the supernatant was used for immunoblot analysis. After the separation of the protein samples on denaturing SDS–PAGE, they were blotted onto polyvinylidene difluoride membrane (Invitrogen). UVR8 and YFP-UVR8 were detected using the anti-UVR8 antibody[55] (kind gift of Roman Ulm, (Geneva, Switzerland) at a dilution of 1:1000 and the subsequent hybridization of the Polyclonal Swine Anti-Rabbit Immunoglobiulins/HRP (Dako) secondary antibody at the dilution of 1:3000. Detection of YFP and GFP-tagged proteins was performed by using an anti-GFP antibody (Clontech), whereas ACTIN was detected by using a monoclonal anti-ACTIN antibody (Sigma-Aldrich) at the dilution of 1:10000 and the subsequent hybridization with the Goat Anti-Mouse igG Peroxidase Conjugated secondary antibody (Invitrogen) at the dilution of 1:10000. Signal visualization was done using Immobilon Western HRP Substrate (Millipore) according to the recommendation of the manufacturer.

Confocal laser scanning microscopy (CLSM). Seeds were surface sterilized and kept in the dark at 4 ºC for 72 h. The seedlings were grown on half-strength Murashige-Skoog medium (Sigma-Aldrich) containing 1% sucrose and 1% agar at 22 ºC under 12h dark/ 12h light regime for 6 days and were irradiated with continuous white light supplemented with UV-B and covered with WG305 or WG385 glass filter as described above for 20 h. CLSM was performed using a Leica SP5 AOBS microscope (Leica) on DMI6000 microscope base using the HC PL APO 20x (NA:0.7) objective lens: with 400 Hz sampling speed; 3x line averaging; 200 µm pinhole; excitation at 488 nm for GFP and at 514 nm for YFP. The spectral emission detectors were set to 496-518 nm for GFP and to 545-582 nm for YFP. Brightness and contrast settings were uniformly done on the corresponding (-UV-B, +UV-B) image pairs. Supplementary Fig. 3 shows that the applied UV-B irradiation does not bleach or enhance the GFP signal.

View Article Online
DOI: 10.1039/C8PP00492G

Hypocotyl length measurement. For hypocotyl length measurements seeds were surface sterilized and placed on half-strength Murashige and Skoog medium supplemented with 1 % sucrose and 0.8% agar[34] and kept at 4 ºC for 72 h. Seeds were germinated at 22 ºC under 12h dark/ 12h light regime for 2 days and seedlings were grown at 22 ºC under the constant irradiation of white light supplemented with or without UV-B as described above for 4 days. The seedlings were placed horizontally on the surface of agar medium and scanned (n=50). The plates were scanned using a flatbed scanner (Epson) and analyzed using MetaMorph Software (Universal Imaging). The relative hypocotyl length, as a ratio of UV-B treated/non-treated hypocotyls were calculated. Experiments were repeated at least three times and the obtained data were plotted on a violin plot using the Seaborn package for Python.

View Article Online
DOI: 10.1039/C8PP00492G

Results

Identification of UVR8 signal reporter transcripts

To identify candidates for universal reporting of UV-B and UVR8 signalling, we used publicly available transcriptome datasets of UV-B regulated genes in photomorphogenic conditions (Table 1). The microarray-based datasets of Brown & Jenkins, 2008; Favory *et al.,* 2009; Oravecz *et al.,* 2006[4,28,52] were chosen to generate a first reference for comparing with other experiments. These transcriptomes are derived from UV-B treated vegetative Arabidopsis plants and contain over 300 UV-B induced genes each. The older similar datasets of Brown *et al.,* 2005; Ulm *et al.,* 2004[6,34] were not included, because of the small coverage of differentially expressed genes. Hence the three datasets for upregulated genes were compared, and a first list of 264 repeatedly UV-B induced genes was generated. This list of 264 genes was then further compared to the RNA-Seq data of root samples of Wan *et al.,* 2018[54], and data from the developing leaf samples of Vandenbussche *et al.,* 2018[53], two studies on photomorphogenic regulation of plant growth by UV-B radiation (Fig. 1). This yielded a set of 42 genes that are induced in all five studies. 87 genes appear in common between the root and leaf study in the RNA-Seq experiments, yet not repeating in the microarray experiments, suggesting these may be the result of higher sensitivity of the RNA-Seq methods. Furthermore, 39 genes are upregulated in seedlings and leaves which could thus function as markers in the shoot. Likewise, 73 genes may be genuine markers for UV-B signalling, and are present in the root. The 1032 genes specific to the Wan *et al.,* dataset may harbour additional root-specific UV-B regulated genes, that were not discovered in seedling tissue because of dilution of the sample and concomitant loss of sensitivity to detect a specific transcript. These would remain to be tested.

View Article Online
DOI: 10.1039/C8PP00492G

Table 1: Studies used to evaluate UV-B regulation of genes

Reference	Sample	UV-B conditions
Oravecz *et al.,* 2006[52]	Seedling	Broadband 15 min 0.12 W m^{-2} UV_{BE*}
Brown and Jenkins. 2008[28]	21-day-old plant	Broadband 4h 3 µmol m^{-2} s^{-1}
Favory *et al.,* 2009[4]	4-day-old seedling	Narrowband 1-6h 1.5 µmol $m^{-2}s^{-1}$
Vandenbussche *et al.,* 2018[53]	21-day-old plant expanding leaf	Broadband 4h 0.7 W m^{-2} (UV-B adapted plants)
Wan *et al.,* 2018[54]	5-day-old seedling root	Narrowband 0.5-2h 1.6 W m^{-2}
Kilian *et al.,* 2007[56]	Seedling	Broadband unfiltered (+UV-C); 1.18 W m^{-2} UV_{BE}
Morales *et al.,* 2013[57]	~3-week-old plant	Solar. 12h of averaged 1.05 µmol m^{-2} s^{-1} UV_{BE}

*BE: Biologically effective

We thus narrowed down candidate markers to 154 (42 overall, 39 shoot only and 73 root only) genes (Supplementary table 2), which we used in a comparison with the UV-B stress dataset of Kilian *et al.,* 2007[56]. It is noteworthy that only 56 genes appeared regulated in common (Supplementary Fig. 4), with many photomorphogenic and flavonoid biosynthesis genes not picked up in the Kilian *et al.,* 2007[56] dataset.

The 154 upregulated genes were further evaluated for UVR8 regulation in the dataset of (Brown *et al.,* 2005; Favory *et al.,* 2009[4,6]. 82 genes could be confirmed as dependent on UVR8 for regulation by UV-B. These are listed in Supplementary table 2.

Next, we compared the 42 overall and the 39 shoot only candidate marker genes for the shoot with the data of Morales *et al.,* who grew plants in the field in the presence or absence of solar UV. 15 genes (Table 2) were found to overlap, suggesting they can be used as candidate markers for UV-B signalling in field studies. Moreover, the regulation of all 15 genes was reported UVR8-dependent in controlled conditions (Table 2). Interestingly, the transcripts of *HY5* and *HYH* were not retrieved as differential in UV-B field conditions, which could be due to masking by expression increases from other wavelength radiation.

View Article Online
DOI: 10.1039/C8PP00492G

Table 2. UV-B upregulated genes found in field conditions

Locus Identifier	Primary Gene Symbol	UVR8-dependent
AT1G06000	(*UGT89C1*)	Yes
AT1G65560		Yes
AT2G37040	*PHE AMMONIA LYASE 1 (PAL1)*	Yes
AT3G22840	*EARLY LIGHT-INDUCABLE PROTEIN (ELIP1)*	Yes
AT3G51240	*FLAVANONE 3-HYDROXYLASE (F3H)*	Yes
AT3G53260	*PHENYLALANINE AMMONIA-LYASE 2 (PAL2)*	Yes
AT3G55120	*TRANSPARENT TESTA 5 (TT5)*	Yes
AT4G14690	*EARLY LIGHT-INDUCIBLE PROTEIN 2 (ELIP2)*	Yes
AT4G31870	*GLUTATHIONE PEROXIDASE 7 (GPX7)*	Yes
AT5G02270	*ATP-BINDING CASSETTE I20 (ABCI20)*	Yes
AT5G05270	*CHALCONE ISOMERASE LIKE (CHIL)*	Yes
AT5G08640	*FLAVONOL SYNTHASE 1 (FLS1)*	Yes
AT5G23730	*REPRESSOR OF UV-B PHOTOMORPHOGENESIS 2 (RUP2)*	Yes
AT5G60540	*PYRIDOXINE BIOSYNTHESIS 2 (PDX2)*	Yes
AT5G62210		Yes

In contrast to the multiple available datasets for UV-B upregulated genes mentioned above, data on downregulated genes is much harder to come by, and sometimes not even mentioned in published records. However, for entire seedlings, one complete set, including downregulated genes, has been published[4]. We compared the UV-B downregulated genes in this set with the UV-B downregulated genes in developing leaves[53], and those in roots[54] (Fig. 2). 9 genes could be universal downregulated UV-B markers, 15 genes are potential shoot specific markers, while 130 are potential root specific markers, yielding a total of 154 downregulated genes (Supplementary table 3). 113 of those appeared to be under UVR8 control. The 24 UV-B downregulated genes in the shoot were compared with the field data of Morales *et al.,* 2013[57]. The comparison of these two small gene lists did not yield any gene in common. This suggests that to date either UV-B-specific downregulated genes still need to be defined by additional experimentation, or UV-B downregulation of genes in controlled conditions does not translate well to field experiments. Gene Ontology (GO) analysis of the upregulated genes confirmed the involvement of flavonoid synthesis (Supplementary table 4), whereas for downregulated genes, primary metabolism appeared to be affected, including respiration and ion transport (Supplementary table 5).

It should be mentioned that in general, preferably a small set of genes should be evaluated, since many genes are responsive to multiple stresses or signals (*e.g.* Morales *et al.,* 2013[57]), and

View Article Online
DOI: 10.1039/C8PP00492G

depending on the situation, candidate marker genes should be screened for induction upon other cues present in an experimental setup.

Reporter genes identify similar and distinct pathways of UVR8 signalling in the shoots and roots

In many of the previously mentioned studies (Table 1) UV-B-irradiated whole seedlings, plants or the aerial parts of the plants were collected for transcriptome analysis. Having small weight of the roots compared with the leaves or cotyledons, transcriptional changes happening in the roots may be masked by mixing different plant organs during sample preparation. In order to compare transcriptional changes in different organs, we collected the roots and the aerial parts of UV-B-irradiated plants separately and measured the expression level of selected reporter genes using qRT-PCR approach. The induction of the well-established *HY5*, *HYH, ELIP2* and *ELIP1* reporters was clearly visible both in the roots and shoots after 2 h of photomorphogenic UV-B irradiation (Fig. 3, Supplementary Figure 5). Involving the *uvr8-6* mutant in the experiment, we also noticed that the measured induction requires functional UVR8 photoreceptor. To test the dependence of the observed transcriptional changes in the root from events occurring in the shoot we developed two approaches. First, we covered the roots of intact plants during the UV-B treatment protecting them from the UV-B. Secondly, we separated the roots from the shoots before the UV-B treatment (Supplementary Figure 2). Interestingly, the reporter induction happened only in those organs of the wild type plants, which were irradiated (*i.e.* was not covered), thus the gene induction occurs both in the roots and the shoots similarly and independently from each other. We also noticed similar gene induction in those organs which were separated from each other during the UV-B irradiation (Fig. 3, Supplementary Figure 5).

Examining randomly selected reporters identified by data mining (Supplementary Table 2), we found a few of them which responded differently in the shoot and root, some of them showing only negligible induction in the root (*GLUTATHIONE PEROXIDASE 7, GPX7*), or in the shoot (*At2g23910*) and also a set of genes which were induced at higher levels in the root than in the shoots. The latter are involved in the synthesis of UV-B protecting flavonoids (*TRANSPARENT TESTA 6* and *5*, *CHALCONE ISOMERASE LIKE*). Our data show that not all examined genes involved in the flavonoid synthesis induced at higher levels in the root: *FLAVONOL SYNTHASE 1* (*FLS1*) is induced similarly in both examined organs. All of these genes respond only when

View Article Online
DOI: 10.1039/C8PP00492G

UV-B directly hits the organ where they are expressed and their UV-B induction is under the control of UVR8 (Fig. 3, Supplementary Figure 5).

HY5-GFP and HYH-GFP are reporters of root UVR8 signalling.

The recent study of Chen *et al.,* 2016[58] reported that HY5-GFP is transported from the shoot to the root under white light illumination. HY5 is a transcription factor with key importance not only in white light but also in UV-B, hence its potential shoot-to-root translocation under UV-B irradiation warrants verification. To address this issue, *pHY5:HY5-GFP* expressing plants were grown on vertical plates and irradiated with photomorphogenic UV-B and their HY5-GFP content was determined in the root and the shoot. UV-B irradiation results in increased HY5-GFP protein accumulation both in root and shoot (Fig. 4A, Supplementary Figure 6A). Furthermore, the lack of such an increase in the *uvr8-6* background indicates that this phenomenon depends on the presence of the UVR8 photoreceptor. Next, we covered the roots of the plants during the UV-B treatment to avoid the effect of direct irradiation on HY5-GFP levels. Covered roots did not contain a higher amount of HY5-GFP than those which were not irradiated with UV-B (Fig. 4A, Supplementary Figure 6A). This observation is strengthened by the result of separately irradiated roots and shoots indicating the need of direct UV-B irradiation to induce higher levels of HY5-GFP accumulation. Interestingly, we got similar results with higher induced protein levels, when we examined the HYH-GFP accumulation in the same experimental system (Fig. 4B, Supplementary Figure 6B). In conclusion, these transcription factors accumulate to high levels under UV-B both in irradiated roots and shoots and we could not detect a major role for shoot-to-root transport in this process.

HY5-GFP and HYH-GFP as a reporter of cell type-specific UVR8 signalling.

Similarly to *HY5*, not only the mRNA level but the protein level of its homologue, *HYH* also increases when UV-B signalling is activated (Figs. 3 and 4). To examine the spatial aspects of this accumulation pattern of the HYH protein we introduced the *pHYH:HYH-GFP* transgene into the *uvr8-6* lines which express the functional YFP-UVR8 protein under the control of its endogenous promoter (*pUVR8:YFP-UVR8)* or specifically in the epidermis (*pML1:YFP-UVR8*) or in the mesophyll and cortex cells (*pCAB3:YFP-UVR8, pC1:YFP-UVR8*) or in the endodermis (*pSCR:YFP-UVR8*). Fig. 5 and Supplementary Fig 7 demonstrate that HYH-GFP is accumulated

View Article Online
DOI: 10.1039/C8PP00492G

in the nuclei and is expressed at low levels in those cells of the hypocotyls which were not irradiated with UV-B. Contrarily, UV-B irradiation leads to HYH-GFP accumulation to high levels, but only in those cells which contain YFP-UVR8, *i.e.* in the epidermis of the *pML1:YFP-UVR8/uvr8-6,* in the cortex of the *pCAB3:YFP-UVR8/uvr8-6* and *pC1:YFP-UVR8/uvr8-6*, in the endodermis of the *pSCR:YFP-UVR8/uvr8-6* and in both the epidermis and cortex of *the pUVR8:YFP-UVR8/uvr8-6* background lines. This finding indicates that the UV-B-induced accumulation of HYH-GFP shows tissue- and cell type autonomous patterns and can be used as a UVR8-dependent cellular marker, similarly to HY5-GFP[44]. We also noted that the induction of HYH-GFP accumulation in the cortex and endodermis indicates that the UVR8 signalling pathways are also active in deeper layers of the hypocotyl (Fig. 5, Supplementary Fig. 7). To extend this observation we also monitored HY5-GFP accumulation in the cortex and endodermis cells of the *pC1:YFP-UVR8/uvr8-6* and *pSCR:YFP-UVR8/uvr8-6* plants in which YFP-UVR8 is expressed only in the cortex and endodermis, respectively. We found that the accumulation pattern of the HY5-GFP shows similar characteristics of the HYH-GFP, *i.e.* photomorphogenic UV-B induces HY5-GFP in those tissues only which express the YFP-UVR8 photoreceptor at high levels (Fig. 6, Supplementary Fig. 8).

Tissues contributing at different levels to the UVR8-regulated inhibition of hypocotyl growth. The output of the UVR8 pathway can be measured by distinct features, of which one of the most frequently referred to is the inhibition of hypocotyl elongation [4,25,33,59,60]. In our previous study we examined cell type specific complementation lines and found that this trait can also be used as a proxy for active UVR8 signalling. We concluded that the epidermal and cortical UVR8 has the main role whereas vascular UVR8 plays a minor role in regulating this response[44]. To extend our findings on particular hypocotyl cell types we characterized this response of the *pC1:YFP-UVR8/uvr8-6* and the *pSCR:YFP-UVR8/uvr8-6* lines expressing YFP-UVR8 in the cortex and endodermis, respectively. Our results show that both lines complement the *uvr8* mutant phenotype, although only to a partial extent (Fig. 7). The *pC1:YFP-UVR8/uvr8-6* line performs better compared to a weak cortical expressor line, *pSUC2:YFP-UVR8/uvr8-6*, but worse than the strong cortex expressor *pCAB3:YFP-UVR8/uvr8-6* suggesting the importance of YFP-UVR8 protein levels in the cortex. The *pSCR:YFP-UVR8/uvr8-6* shows weak complementation indicating that the role of UVR8 in the endodermis is minor in the inhibition of hypocotyl elongation, similarly to the vascular UVR8 in the *pSUC2:YFP-UVR8/uvr8-6* (reference[44] and Fig. 7). This conclusion is supported by the response of the *pML1:YFP-UVR8/uvr8-6* which contains similar

View Article Online
DOI: 10.1039/C8PP00492G

amount of YFP-UVR8 than the *pSCR:YFP-UVR8/uvr8-6* and less than the *pSUC2:YFP-UVR8/uvr8-6* line but its epidermal YFP-UVR8 triggers more effective response than higher amounts in the depth of the plant body. These data indicate that hypocotyl elongation inhibition can be used as a qualitative measure for assessing the presence of a UVR8 signal in different cell types, especially when those cell types overlap with the expression pattern of the endogenous promoter.

Local signal tracking: Flavonoid accumulation to report UVR8 signal. When exposed to UV-B, wild type plants have a strongly upregulated flavonol biosynthesis[26]. Previous studies indicated that the epidermis and mesophyll tissues of the cotyledon are important for UV-B perception in seedlings[44]. We examined the location of flavonoid accumulation in the upper part of the hypocotyl of 5-day-old seedlings, exposed to 1 μmol m^{-2} s^{-1} 311 nm adaxial UV-B for 3 days. In wild type plants, there is clear UVR8-dependent accumulation of flavonoids, among them the DPBA-kaempferol complex is visible by green fluorescence after DPBA staining[61] in the epidermal cell layer. Identical observations are made for *uvr8-6* mutant background plants expressing the YFP-UVR8 fusion protein under its endogenous promoter (*pUVR8:YFP-UVR8*) and under the control of an epidermis-specific promoter (*pML1:YFP-UVR8*), consistent with the latter plants only expressing UVR8 in the epidermal cell layers (Fig. 5). Interestingly, while *pUVR8:YFP-UVR8* is also expressed in the inner cortical layer, no flavonoids could be detected in this cell layer. Nevertheless, flavonoid production can be induced in the outer cortical layer, as observed in two reporter lines having YFP-UVR8 expression in cortical cell layers (transgenes: *pCAB3:YFP-UVR8, pC1:YFP-UVR8*). Interestingly, the inner cortical layer of these lines does not accumulate detectable amount of flavonoids, despite expressing YFP-UVR8 (Fig. 8). Surprisingly, deeper layers such as the endodermis and the vasculature can also accumulate flavonoids upon UV-B exposure, when UVR8 is specifically expressed in that region in the *pSCR:YFP-UVR8/uvr8-6* and *pSUC2:YFP-UVR8/uvr8-6* lines, respectively.

Discussion

Markers for signalling pathways are very handy tools to dissect complex biological processes from subcellular to whole plant level. In this work we identified a number of suitable markers that can be used for detecting UV-B photomorphogenic processes dependent on the specific photoreceptor UVR8. A meta-analysis of publicly available UV-B-regulated transcriptomes and

View Article Online
DOI: 10.1039/C8PP00492G

their dependence of UVR8 led to a compilation of recurring genes regulated by UVR8 (Supplementary Tables 2 and 3). All of the UVR8 reporter genes frequently used today and mentioned in the introduction were recovered in the final gene lists (Supplementary tables 2 and 3), except for At1g16260 (WAKL8), and rather surprisingly At5g13930 (CHS), which appears in seedling samples, yet not in the UV-B-upregulated transcriptome of roots or developing leaves of UV-B adapted plants and was therefore not withheld in the final list (Supplementary table 2). There are several possible, and mutually not exclusive explanations: (i) gene induction of different genes requires different length of UV-B treatment, (ii) not all UV-B regulated genes can be universally used as UVR8 markers and (iii) some markers may be confined to use at particular developmental stages or plant organs. Moreover, a notable shortcoming of the currently available transcriptome datasets is that they are mostly derived from seedlings and shoots, whereas only one root-specific dataset is available[54]. Additional transcriptome profiling experiments on root tissue would be of great interest to understand the processes that can be UV-B activated or repressed in roots. Such studies could help explaining potential differences between root and shoot regulation by UVR8, some of which discovered here by qRT-PCR (Fig. 3, Supplementary Fig. 5). Furthermore, caution should be taken with the use of single genes as markers for a specific process. For instance, in the case of genes in the flavonoid biosynthesis pathway, gene regulatory overlaps exist with other light signalling pathways and abiotic stresses[62,63]. It is therefore advisable to use a gene set representing distinct UV-B controlled output processes to diagnose the activity of the UVR8 pathway. As a starting point to build such a diagnostic gene set for Arabidopsis, we propose to use (a selection of) those presented in Table 2 as a base, as these markers for UVR8 signalling are useable in outdoor conditions, where many other gene regulating cues are present. This set can be extended with *HY5* and *HYH*, and additional genes of choice from the lists in Supplementary table 2 and 3, such as *SIG5* and *At2g23910* (Fig. 3, Supplementary Fig. 5).

The best markers and reporters are those that can also be used beyond one species of interest. The UV-B regulation of flavonoid biosynthesis appears a widespread process among plants, hence suitable for harbouring candidate biological markers. Some of the marker genes that control flavonoid biosynthesis are put forward here, have already been shown to have functional homo- or orthologues in other species. They include *HY5, HYH, F3H, FLS*, members of the MYB family[64-66]. Therefore, the extended list of genes (Table 2, Supplementary table 2 and 3) will be a solid base for the identification of functionally homologous gene sets across species. Beyond the transcript level, the protein levels of UVR8-controlled transcription factors are also good indicators for photoreceptor activity (Fig. 4-6). Finally, the use of flavonoid accumulation as quantitative

View Article Online
DOI: 10.1039/C8PP00492G

parameter for UV-B signal in plant extracts cannot be disputed. However, monitoring the DPBA-flavonoid complex accumulation by CLSM has its limits. It is suitable at whole plant and organ level, but not as marker for cell type specific responses, as its tissue-type accumulation pattern does not exactly follow the spatial distribution of UVR8 expression in hypocotyls (Fig. 8).

To put the validity of markers for monitoring UVR8-triggered responses to the test, we characterized the UV-B response of selected reporters (Fig. 3, Supplementary Fig. 5). The differences between the induction in the shoots and roots indicate that besides the same molecular pathways, organ-specific pathways are also existing and activated. The similar upregulation of the key transcription factors, *HY5* and *HYH,* suggests that the first step of UVR8 signalling happens similarly both in the shoot and the root. Notwithstanding this conclusion we also note, that the downstream signalling steps including the regulation of genes involved in flavonoid synthesis show characteristic differences between the shoot and root. Involvement of differently expressed flavonoid synthesis genes gives the possibility of regulating processes like root development, gravitropism and phototropism, auxin transport by fine-tuning flavonoid levels in the root and shoot[67-69].

It is a common feature of all examined UVR8-dependent reporters, that for transcription induction they require the presence of the UV-B photoreceptor in the same organ (root or shoot, Fig.3, Supplementary Fig. 5). This finding lets us draw the following conclusions: firstly, there is no obvious light pipe effect which directs sufficient UV-B radiation from the aerial parts of the plants to the roots to trigger the observed responses. This biological system may behave differently when compared to dark-adapted seedlings in which the light is transferred down to the roots via the hypocotyl[46,70]. Etiolated tissues contain less light-blocking chromatic compounds inhibiting the light passing through, whereas in light-grown tissues the accumulation of secondary metabolites in the shoot is an additional barrier for efficient light penetration in seedlings. Additionally, the higher energy UV-B photons are absorbed in the tissues with higher probability than the low energy red or far-red photons[71]. Secondly, our results suggest, that the inter-organ transfer of signalling molecules (including the mRNAs of the reporters) from the shoot to the root do not alter significantly the observed gene induction responses. Furthermore, the accumulation of HYH-GFP and HY5-GFP fusion protein was elevated only in those tissues which were irradiated directly with UV-B. This response happened even in separated roots and shoots of only those plants which possess UVR8 (Fig. 4, Supplementary Fig. 6). Thus we assume that the accumulation of these transcription factors is controlled differently under UV-B than under white light where shoot-to-root HY5 transport was observed[58]. At this point, we cannot exclude the possibility that different

View Article Online
DOI: 10.1039/C8PP00492G

regulations are active under the control of different photoreceptors (*i.e.* irradiation with different spectral composition), furthermore parallel processes (transport and synthesis) can also co-exist under UV-B, being the synthesis the dominant one. This observation nicely corroborates the findings of Zhang et al[72]. Thus, our data suggest that the early steps of the UVR8-regulated pathways functions similarly in roots and shoots including the transcriptional and translational regulation of key transcription factors but later steps of the signalling differ leading to altered transcriptional responses (Figs. 3 and 4, Supplementary Figs. 5 and 6). A recent study shows that HY5 signalling in the shoot controls the development of root primordia in white and far-red light[73] . Although these authors did not determine the total HY5 amount in different organs or the possible inter-organ transport of HY5, this finding indicates that signalling between the shoot and root has multiple facets thus could be the subject of further studies. These include the examination of the signalling pathways under the control of different photoreceptors and the elaboration of their functionality in certain parts/sections of the root and shoot.

Our results show that both HY5 and HYH are excellent reporters for UVR8 signalling in laboratory conditions. Induction of *HY5* and *HYH* transcript increase in UV-B was identified as an early photomorphogenic UV-B response. The importance of these genes in the development of UV-B protection and also UV-B-induced signalling pathways were also examined revealing that their function is redundant, and *HY5* has the main role and *HYH* has only minor[28,74] . We also noticed, that the induction of HYH protein accumulation is higher than that of HY5 (Fig. 4, Supplementary Fig. 6). Together with the more pronounced role of HY5 in the so far examined responses, this observation indicates that HYH may have a specific, yet unidentified role in UV-B signalling. Not only the accumulation of the GFP fusion proteins of HY5 and HYH can be used in both roots and shoots as markers but HYH-GFP and HY5-GFP are also suitable markers for tracing tissue-dependent characteristics of UV-B signalling (Figs. 4-6). They behave similarly showing clear UVR8-dependent, tissue-specific induction in the hypocotyl cells under photomorphogenic UV-B. This finding is in harmony with the results obtained from cotyledon cells[44] suggesting universal spatial regulatory patterns throughout different organs. Targeted induction of HY5 by expressing YFP-UVR8 in different tissues show a similar pattern with the flavonoid accumulation in these lines. HY5-GFP, HYH-GFP and flavonoid accumulation can be induced in those tissues (*e.g.* vasculature and endodermis) where *pUVR8* cannot produce detectable amount of YFP-UVR8 simply by expressing the UV-B photoreceptor using tissue-specific promoters, such as *pSUC2* and *pSCR* (Figs. 5 and 8). Analysing these reporters, we note that their induction indicates that UV-B reaches even the most hidden inner tissues of the hypocotyls. Furthermore, the wild type Columbia lines contain undetectable flavonoid levels in these tissues suggesting that despite

View Article Online
DOI: 10.1039/C8PP00492G

UVR8 signalling pathway elements can be found in these cells, these compounds accumulate mainly in the cells closer to the surface, not in the depth of the plant body under photomorphogenic UV-B irradiation. The endogenous *pUVR8* promoter also drives expression of UVR8 in the outer cortical layer, while no green DPBA-flavonoid staining is detected there, indicating, that the accumulation of the DPBA-flavonoid complex is not ideal as marker for a UVR8 signal within an organ. We speculate that high UVR8 protein level is required for detectable cortical flavonoid accumulation as in the *pCAB3:YFP-UVR8/uvr8-6* and *pC1:YFP-UVR8/uvr8-6* lines but not in the lower cortical expressor *pUVR8:YFP-UVR8/uvr8-6*[44]. In fact, flavonoids, mainly kaempferol accumulation in the hypocotyl shows tissue-autonomous characteristics, restricted to that cell layer, where UVR8 is expressed at high levels (Fig. 8). We notice, that those plants expressing YFP-UVR8 at high levels in both the inner and outer cells of the hypocotyl, are not able to accumulate flavonoids in the inner layers, whereas those which contain low levels of UVR8 in the outer layers can. We speculate, that this may be due to an inward directed inter-cell layer specific signal that regulates the biosynthesis of flavonoids causing a block of flavonoid production in inner layers. Alternatively, a screening effect of outer cell layers by accumulating UV-absorbing pigments over the inner layers could also cause reduced flavonoid aggregation in the inner layers. These theories could explain the high levels of accumulated flavonoids in the endodermis and vasculature in the *pSCR:YFP-UVR8/uvr8-6* and *pSUC2:YFP-UVR8/uvr8-6* seedlings, which do not contain detectable amounts of UVR8 in their epidermis.

Our results also demonstrate that the artificially induced high level UVR8 signalling in the endodermis results in elevated HYH, HY5 and flavonoid accumulation locally, but does not lead to the inhibition of hypocotyl growth, in contrast with when UVR8 is expressed in the epidermis (Figs. 7 and 8). These results corroborate those observations which indicate that vascular UVR8 has a negligible effect on hypocotyl elongation[44]. In conclusion, we can assume that targeted UVR8 expression results in gene expressional changes and flavonoid accumulation in different tissues, but to achieve proper growth responses, UVR8 signalling in tissues closer to the surface of the plant body (cortex, epidermis) is required. This is in accordance with other findings indicating the accentuated role of the outer layers of plant shoot in growth control[75,76].

Conclusions

Many studies examine the effect of UV-B on higher plants. Here we focused on responses initiated by photomorphogenic UV-B which are dominantly transmitted by the UVR8 photoreceptor. Examining different responses and performing extensive data mining we show how different

View Article Online
DOI: 10.1039/C8PP00492G

reporters of UVR8 signalling can be developed and used. We found that transcriptomic and protein accumulation responses indicate that there are independent signalling pathways in the root and shoot possessing similar and different molecular components. By examining other complex phenotypic responses such as the accumulation of UV-B protecting flavonoids or the inhibition of hypocotyl elongation triggered by UV-B we can identify the contribution of different tissue and cell types and we can monitor the nature of signal spreading between these tissues. Our investigations also provide data about the mechanisms of the UVR8-governed signalling pathways in different tissues and contribute to the long since examined UV-B intrusion into the tissue layers located in the depth of the plant body.

Conflicts of interest

There are no conflicts to declare.

Acknowledgements

We thank Dr. Tivadar Danka for the help with the violin plot. This work was supported by the international collaboration project of the research foundation Flanders (FWO) and the Hungarian Academy of Sciences VS.074.16N to F.V., D.V.D.S. and A.V., an FWO Research Grant to F.V. (G000515N), and support from Ghent University to D.V.D.S.. L.V. is a pre-doctoral fellow of the Research Foundation Flanders (FWO). The work in Hungary was supported by grants from the Economic Development and Innovation Operative Program (GINOP-2.3.2-15-2016-00015 and GINOP-2.3.2-15-2016-00032).

Electronic supplementary information (ESI) available:

Supplementary table 1
Oligonucleotides used in qRT-PCR assays
Supplementary table 2
UV-B upregulated genes identified in the examined transcriptome datasets
Supplementary table 3
UV-B downregulated genes identified in the examined transcriptome datasets
Supplementary table 4

View Article Online
DOI: 10.1039/C8PP00492G

GENE Ontology (GO) categories of the UVR8-dependent upregulated genes shown in Supplementary table 2.

Supplementary table 5

GENE Ontology (GO) categories of the UVR8-dependent downregulated genes shown in Supplementary table 3.

Supplementary Figure. 1.

Venn diagram of *Arabidopsis* UV-B upregulated genes taken from lists as published in Favory *et al.,* 2009, Oravecz *et al.,* 2006 and Brown and Jenkins, 2008.

Supplementary Figure 2.

Schematic diagram of the performed irradiation and dissection protocols

Supplementary Figure 3.

The GFP signal is not altered by the applied UV-B irradiation.

Supplementary Figure. 4.

Venn diagram of *Arabidopsis* UV-B upregulated genes listed in Supplementary table 2, showing overlap with the stress UV-B dataset from Kilian *et al.,* 2007.

Supplementary Figure 5.

Reporters of transcriptional changes in different plant organs.

Supplementary Figure 6.

Accumulation of HY5-GFP and HYH-GFP in different organs of Arabidopsis seedlings under UV-B irradiation.

Supplementary Figure 7.

UV-B induction of *pHYH:HYH-GFP* in the hypocotyl cells of transgenic lines expressing YFP-UVR8 in different tissues.

Supplementary Figure 8.

UV-B induced accumulation of HY5-GFP in the hypocotyl cells of transgenic lines expressing YFP-UVR8 in different tissues.

Supplementary Figure 9.

Expression levels of YFP-UVR8 in different transgenic lines.

View Article Online
DOI: 10.1039/C8PP00492G

References

1. A. B. Britt, *Annual Review of Plant Physiology and Plant Molecular Biology*, 1996, **47**, 75-100.
2. P. Casati and V. Walbot, *Plant physiology*, 2003, **132**, 1739-1754.
3. E. Hideg, M. A. Jansen and A. Strid, *Trends in plant science*, 2013, **18**, 107-115.
4. J. J. Favory, A. Stec, H. Gruber, L. Rizzini, A. Oravecz, M. Funk, A. Albert, C. Cloix, G. I. Jenkins, E. J. Oakeley, H. K. Seidlitz, F. Nagy and R. Ulm, *The EMBO journal*, 2009, **28**, 591-601.
5. D. J. Kliebenstein, J. E. Lim, L. G. Landry and R. L. Last, *Plant physiology*, 2002, **130**, 234-243.
6. B. A. Brown, C. Cloix, G. H. Jiang, E. Kaiserli, P. Herzyk, D. J. Kliebenstein and G. I. Jenkins, *Proceedings of the National Academy of Sciences of the United States of America*, 2005, **102**, 18225-18230.
7. L. Rizzini, J. J. Favory, C. Cloix, D. Faggionato, A. O'Hara, E. Kaiserli, R. Baumeister, E. Schafer, F. Nagy, G. I. Jenkins and R. Ulm, *Science*, 2011, **332**, 103-106.
8. G. I. Jenkins, *Plant, cell & environment*, 2017, **40**, 2544-2557.
9. J. M. Christie, A. S. Arvai, K. J. Baxter, M. Heilmann, A. J. Pratt, A. O'Hara, S. M. Kelly, M. Hothorn, B. O. Smith, K. Hitomi, G. I. Jenkins and E. D. Getzoff, *Science*, 2012, **335**, 1492-1496.
10. D. Wu, Q. Hu, Z. Yan, W. Chen, C. Yan, X. Huang, J. Zhang, P. Yang, H. Deng, J. Wang, X. Deng and Y. Shi, *Nature*, 2012, **484**, 214-219.
11. T. Mathes, M. Heilmann, A. Pandit, J. Zhu, J. Ravensbergen, M. Kloz, Y. Fu, B. O. Smith, J. M. Christie, G. I. Jenkins and J. T. Kennis, *J Am Chem Soc*, 2015, **137**, 8113-8120.
12. X. Li, L. W. Chung, K. Morokuma and G. Li, *J Chem Theory Comput*, 2014, **10**, 3319-3330.
13. A. A. Voityuk, R. A. Marcus and M. E. Michel-Beyerle, *Proceedings of the National Academy of Sciences of the United States of America*, 2014, **111**, 5219-5224.
14. M. Wu, A. Strid and L. A. Eriksson, *J Phys Chem B*, 2014, **118**, 951-965.
15. Z. Liu, X. Li, F. W. Zhong, J. Li, L. Wang, Y. Shi and D. Zhong, *J Phys Chem Lett*, 2014, **5**, 69-72.
16. M. Heilmann, J. M. Christie, J. T. Kennis, G. I. Jenkins and T. Mathes, *Photochem Photobiol Sci*, 2015, **14**, 252-257.
17. T. Miyamori, Y. Nakasone, K. Hitomi, J. M. Christie, E. D. Getzoff and M. Terazima, *Photochem Photobiol Sci*, 2015, **14**, 995-1004.
18. X. Zeng, Z. Ren, Q. Wu, J. Fan, P. P. Peng, K. Tang, R. Zhang, K. H. Zhao and X. Yang, *Nat Plants*, 2015, **1**.
19. X. Huang, X. Ouyang and X. W. Deng, *Curr Opin Plant Biol*, 2014, **21**, 96-103.
20. O. S. Lau and X. W. Deng, *Trends in plant science*, 2012, **17**, 584-593.
21. D. Zhu, A. Maier, J. H. Lee, S. Laubinger, Y. Saijo, H. Wang, L. J. Qu, U. Hoecker and X. W. Deng, *The Plant cell*, 2008, **20**, 2307-2323.
22. M. T. Osterlund, C. S. Hardtke, N. Wei and X. W. Deng, *Nature*, 2000, **405**, 462-466.
23. X. Huang, X. Ouyang, P. Yang, O. S. Lau, L. Chen, N. Wei and X. W. Deng, *Proceedings of the National Academy of Sciences of the United States of America*, 2013, **110**, 16669-16674.
24. M. Binkert, L. Kozma-Bognar, K. Terecskei, L. De Veylder, F. Nagy and R. Ulm, *The Plant cell*, 2014, **26**, 4200-4213.

View Article Online
DOI: 10.1039/C8PP00492G

25. Y. Yang, T. Liang, L. Zhang, K. Shao, X. Gu, R. Shang, N. Shi, X. Li, P. Zhang and H. Liu, *Nature*, 2018, **4**, 98-107.
26. R. Stracke, O. Jahns, M. Keck, T. Tohge, K. Niehaus, A. R. Fernie and B. Weisshaar, *The New phytologist*, 2010, **188**, 985-1000.
27. M. Heijde and R. Ulm, *Trends in plant science*, 2012, **17**, 230-237.
28. B. A. Brown and G. I. Jenkins, *Plant physiology*, 2008, **146**, 576-588.
29. L. Liu, S. Gregan, C. Winefield and B. Jordan, *Plant, cell & environment*, 2015, **38**, 905-919.
30. W. A. Clayton, N. W. Albert, A. H. Thrimawithana, T. K. McGhie, S. C. Deroles, K. E. Schwinn, B. A. Warren, A. R. G. McLachlan, J. L. Bowman, B. R. Jordan and K. M. Davies, *The Plant journal : for cell and molecular biology*, 2018, DOI: 10.1111/tpj.14044.
31. C. Cloix and G. I. Jenkins, *Molecular plant*, 2008, **1**, 118-128.
32. V. Moriconi, M. Binkert, C. Costigliolo, R. Sellaro, R. Ulm and J. J. Casal, *Plant physiology*, 2018, **177**, 75-81.
33. R. Yin, A. B. Arongaus, M. Binkert and R. Ulm, *The Plant cell*, 2015, **27**, 202-213.
34. R. Ulm, A. Baumann, A. Oravecz, Z. Mate, E. Adam, E. J. Oakeley, E. Schafer and F. Nagy, *Proceedings of the National Academy of Sciences of the United States of America*, 2004, **101**, 1397-1402.
35. T. A. Day, G. Martin and T. C. Vogelman, *Plant, cell & environment*, 1993.
36. P. W. Barnes, S. D. Flint, R. J. Ryel, M. A. Tobler, A. E. Barkley and J. J. Wargent, *Plant physiology and biochemistry : PPB*, 2015, **93**, 94-100.
37. L. A. Diaz-Ramos, A. O'Hara, S. Kanagarajan, D. Farkas, A. Strid and G. I. Jenkins, *Photochem Photobiol Sci*, 2018, **17**, 1108-1117.
38. T. Preuten, T. Hohm, S. Bergmann and C. Fankhauser, *Current biology : CB*, 2013, **23**, 1934-1938.
39. K. Yamamoto, T. Suzuki, Y. Aihara, K. Haga, T. Sakai and A. Nagatani, *Plant and Cell Physiology*, 2014, **55**, 497-506.
40. F. Vandenbussche and D. Van Der Straeten, *Plant physiology*, 2014, **166**, 40-43.
41. M. Endo, N. Mochizuki, T. Suzuki and A. Nagatani, *The Plant cell*, 2007, **19**, 84-93.
42. D. Kirchenbauer, A. Viczian, E. Adam, Z. Hegedus, C. Klose, M. Leppert, A. Hiltbrunner, S. Kircher, E. Schafer and F. Nagy, *The New phytologist*, 2016, **211**, 584-598.
43. M. Endo, S. Nakamura, T. Araki, N. Mochizuki and A. Nagatani, *The Plant cell*, 2005, **17**, 1941-1952.
44. P. Bernula, C. D. Crocco, A. B. Arongaus, R. Ulm, F. Nagy and A. Viczian, *Plant, cell & environment*, 2017, **40**, 1104-1114.
45. J. Kim, K. Song, E. Park, K. Kim and G. Bae, *Plantcell*, 2016, **28**, 2770-2785.
46. H. J. Lee, J. H. Ha, S. G. Kim, H. K. Choi, Z. H. Kim, Y. J. Han, J. I. Kim, Y. Oh, V. Fragoso, K. Shin, T. Hyeon, H. G. Choi, K. H. Oh, I. T. Baldwin and C. M. Park, *Science signaling*, 2016, **9**, ra106.
47. H. G. Nimmo, *Plant, cell & environment*, 2018, **41**, 1742-1748.
48. P. Casati and V. Walbot, *Genome biology*, 2004, **5**, R16.
49. M. Karimi, A. Bleys, R. Vanderhaeghen and P. Hilson, *Plant physiology*, 2007, **145**, 1183-1191.
50. Z. Magyar, B. Horvath, S. Khan, B. Mohammed, R. Henriques, L. De Veylder, L. Bako, B. Scheres and L. Bogre, *The EMBO journal*, 2012, **31**, 1480-1493.
51. J. C. Oliveros, Venny. An interactive tool for comparing lists with Venn's diagrams., http://bioinfogp.cnb.csic.es/tools/venny/index.html).
52. A. Oravecz, A. Baumann, Z. Mate, A. Brzezinska, J. Molinier, E. J. Oakeley, E. Adam, E. Schafer, F. Nagy and R. Ulm, *The Plant cell*, 2006, **18**, 1975-1990.

View Article Online
DOI: 10.1039/C8PP00492G

53. F. Vandenbussche, N. Yu, W. Li, L. Vanhaelewyn, M. Hamshou, D. Van Der Straeten and G. Smagghe, *Plant science : an international journal of experimental plant biology*, 2018, **268**, 54-63.
54. J. Wan, P. Zhang, R. Wang, L. Sun, W. Wang, H. Zhou and J. Xu, *Frontiers in plant science*, 2018, **9**, 618.
55. M. Heijde and R. Ulm, *Proceedings of the National Academy of Sciences of the United States of America*, 2013, **110**, 1113-1118.
56. J. Kilian, D. Whitehead, J. Horak, D. Wanke, S. Weinl, O. Batistic, C. D'Angelo, E. Bornberg-Bauer, J. Kudla and K. Harter, *The Plant journal : for cell and molecular biology*, 2007, **50**, 347-363.
57. L. O. Morales, M. Brosche, J. Vainonen, G. I. Jenkins, J. J. Wargent, N. Sipari, A. Strid, A. V. Lindfors, R. Tegelberg and P. J. Aphalo, *Plant physiology*, 2013, **161**, 744-759.
58. X. Chen, Q. Yao, X. Gao, C. Jiang, N. P. Harberd and X. Fu, *Current biology : CB*, 2016, **26**, 640-646.
59. G. Soriano, C. Cloix, M. Heilmann, E. Nunez-Olivera, J. Martinez-Abaigar and G. I. Jenkins, *The New phytologist*, 2018, **217**, 151-162.
60. T. Liang, S. Mei, C. Shi, Y. Yang, Y. Peng, L. Ma, F. Wang, X. Li, X. Huang, Y. Yin and H. Liu, *Developmental cell*, 2018, **44**, 512-523 e515.
61. R. Stracke, H. Ishihara, G. Huep, A. Barsch, F. Mehrtens, K. Niehaus and B. Weisshaar, *The Plant journal : for cell and molecular biology*, 2007, **50**, 660-677.
62. F. Vandenbussche, Y. Habricot, A. S. Condiff, R. Maldiney, D. Van der Straeten and M. Ahmad, *The Plant journal : for cell and molecular biology*, 2007, **49**, 428-441.
63. E. Georgii, M. Jin, J. Zhao, B. Kanawati, P. Schmitt-Kopplin, A. Albert, J. B. Winkler and A. R. Schaffner, *BMC plant biology*, 2017, **17**, 120.
64. R. A. Henry-Kirk, B. Plunkett, M. Hall, T. McGhie, A. C. Allan, J. J. Wargent and R. V. Espley, *Plant, cell & environment*, 2018, **41**, 675-688.
65. Z. Liu, Y. Liu, Z. Pu, J. Wang, Y. Zheng, Y. Li and Y. Wei, *Biotechnology letters*, 2013, **35**, 1765-1780.
66. S. Czemmel, J. Holl, R. Loyola, P. Arce-Johnson, J. A. Alcalde, J. T. Matus and J. Bogs, *Frontiers in plant science*, 2017, **8**, 1084.
67. C. S. Buer, F. Kordbacheh, T. T. Truong, C. H. Hocart and M. A. Djordjevic, *Planta*, 2013, **238**, 171-189.
68. W. Grunewald, I. De Smet, D. R. Lewis, C. Lofke, L. Jansen, G. Goeminne, R. Vanden Bossche, M. Karimi, B. De Rybel, B. Vanholme, T. Teichmann, W. Boerjan, M. C. Van Montagu, G. Gheysen, G. K. Muday, J. Friml and T. Beeckman, *Proceedings of the National Academy of Sciences of the United States of America*, 2012, **109**, 1554-1559.
69. C. S. Buer and M. A. Djordjevic, *Journal of experimental botany*, 2009, **60**, 751-763.
70. A. Kakuszi, E. Sarvari, A. Solti, G. Czegeny, E. Hideg, E. Hunyadi-Gulyas, K. Boka and B. Boddi, *Journal of photochemistry and photobiology. B, Biology*, 2016, **161**, 422-429.
71. C. Markstadter, I. Queck, J. Baumeister, M. Riederer, U. Schreiber and W. Bilger, *Photosynthesis research*, 2001, **67**, 17-25.
72. Y. Zhang, C. Li, J. Zhang, J. Wang, J. Yang, Y. Lv, N. Yang, J. Liu, X. Wang, G. Palfalvi, G. Wang and L. Zheng, *PLoS One*, 2017, **12**, e0180449.
73. K. van Gelderen, C. Kang, R. Paalman, D. Keuskamp, S. Hayes and R. Pierik, *The Plant cell*, 2018, **30**, 101-116.
74. R. Stracke, J. J. Favory, H. Gruber, L. Bartelniewoehner, S. Bartels, M. Binkert, M. Funk, B. Weisshaar and R. Ulm, *Plant, cell & environment*, 2010, **33**, 88-103.
75. Vaseva, II, E. Qudeimat, T. Potuschak, Y. Du, P. Genschik, F. Vandenbussche and D. Van Der Straeten, *Proceedings of the National Academy of Sciences of the United States of America*, 2018, **115**, E4130-E4139.
76. S. Savaldi-Goldstein, C. Peto and J. Chory, *Nature*, 2007, **446**, 199-202.

View Article Online
DOI: 10.1039/C8PP00492G

FIGURE LEGENDS

Fig. 1. Comparison of UV-B upregulated genes throughout different datasets. (**A**) Venn diagram of UV-B upregulated genes selected from the Brown & Jenkins, 2008; Favory *et al.,* 2009; Oravecz *et al.,* 2006 datasets (BFO)[4, 28, 52], as well as those from developing leaves (Vandenbussche *et al.,* 2018[53]) and roots (Wan *et al.,* 2018[54]). (**B**) Venn diagram comparing UV-B upregulated genes in the shoot in controlled conditions (Shoot) with the UV-B upregulated genes from the field experiment of Morales *et al.,* 2013[57].

Fig. 2. Comparison of UV-B downregulated genes throughout different datasets. Venn diagram of UV-B downregulated genes selected from the Favory *et al.,* 2009 dataset[4], as well as those from developing leaves (Vandenbussche *et al.,* 2018 [53]) and roots (Wan *et al.,* 2018 [54]) datasets.

Fig. 3. Reporters of transcriptional changes in different plant organs. Columbia wild type and *uvr8-6* plants were grown on vertical plates for 11 days and were irradiated with white light supplemented with UV-B or not supplemented for 2 h. Roots and shoots of the plants were collected separately. Samples from plants with roots covered during (COVER) or from plants with roots and shoots separated before the UV-B treatment (CUT) were also collected and analysed by qRT-PCR after total RNA extraction. The signals were normalized to the corresponding *TUBULIN* signal and relative values were determined (UV-B treated/non-treated plants). Error bars indicate standard error (n=3).

Fig. 4. Accumulation of HY5-GFP and HYH-GFP in different organs of Arabidopsis seedlings under UV-B irradiation. Columbia wild type and *uvr8-6* plants expressing *pHY5:HY5-GFP* (panel A) or *pHYH:HYH-GFP* (panel B) were grown on vertical plates for 10 days and were irradiated with white light supplemented with UV-B (+UV-B) or not supplemented (-UV-B) for 20h. Roots or shoots (aerial parts) of the plants were collected separately. Samples from plants with roots covered during (COVER) or from plants with roots and shoots separated before the UV-B treatment (CUT) were also collected. The protein extracts were tested with western blot analysis using anti-GFP antibody to visualize bands corresponding to HY5-GFP (panel A) and HYH-GFP (panel B) whereas hybridization with anti-ACTIN antibody was performed to check the amount of protein present in the lanes. Signals corresponding to the HY5-GFP and HYH-GFP bands were quantified, normalized to the corresponding ACTIN signal. The -UV-B samples in both organs and both genotypes were set to 100%.

View Article Online
DOI: 10.1039/C8PP00492G

Fig. 5. UV-B induction of *pHYH:HYH-GFP* in the hypocotyl cells of transgenic lines expressing YFP-UVR8 in different tissues. *pHYH:HYH-GFP* was introduced into Columbia (Col) wild type and into transgenic *uvr8-6* lines expressing *pUVR8:YFP-UVR8*, *pML1:YFP-UVR8, pCAB3:YFP-UVR8, pC1:YFP-UVR8* or *pSCR:YFP-UVR8*. Localization of the HYH-GFP (green colour) and the YFP-UVR8 (red colour) fusion proteins were monitored by CLSM. The focal planes were set on the epidermis, cortex or endodermis cells of the hypocotyl of 6-day-old seedlings irradiated with constant WL supplemented with UV-B (+UV-B) or not supplemented (-UV-B) for 20 h. Identical microscope settings were used to allow determination of the difference between the visual signals of the +UV-B and –UV-B image pairs. White, yellow and red arrows indicate the positions of selected nuclei containing HYH-GFP signal in the epidermis, cortex and endodermis, respectively. Scale bars indicate 100 μm.

Fig. 6. UV-B induced accumulation of HY5-GFP in the hypocotyl cells of transgenic lines expressing YFP-UVR8 in different tissues. *pHY5:HY5-GFP* was introduced into transgenic *uvr8-6* lines expressing *pC1:YFP-UVR8* (panel A) or *pSCR:YFP-UVR8* (panel B). Localization of the HY5-GFP (green colour) and the YFP-UVR8 (red colour) fusion proteins were monitored by CLSM. The focal planes were set on the epidermis, cortex and endodermis cells of the hypocotyl of 6-day-old seedlings irradiated with constant WL supplemented with UV-B (+UV-B) or not supplemented (-UV-B) for 20 h. Identical microscope settings were used to allow determination of the difference between the visual signals of the +UV-B and –UV-B image pairs. White, yellow and red arrows indicate the positions of selected nuclei containing HYH-GFP signal in the epidermis, cortex and endodermis, respectively. Scale bars indicate 100 μm.

Fig. 7. Expression of YFP-UVR8 in different tissues contributes differently to hypocotyl elongation inhibition. A Seedlings were grown under constant white light supplemented with or without 1.5 μmol m^{-2} s^{-1} UV-B. Their hypocotyl length was measured and the relative hypocotyl length values were calculated and spotted. Together with the wild type Columbia (Col) *uvr8-6* mutant and *uvr8-6* mutant expressing *pUVR8:YFP-UVR8* (pUVR8). *pML1:YFP-UVR8* (pML1), *pCAB3:YFP-UVR8* (pCAB3), *pSUC2:YFP-UVR8* (pSUC2), *pC1:YFP-UVR8* (pC1), *pSCR:YFP-UVR8* (pSCR) transgenes were included in the assay. Each measurement was repeated at least 3 times. Asterisks mark lines that display significant differences as compared with the *uvr8-6* mutant line calculated by the Student's t-test (significance: ***P< 0.005). **B.** Seedlings were grown under constant WL supplemented with UV for 7 days before total protein extraction. The protein extracts were tested with western blot analysis using anti-UVR8 antibody to visualize bands corresponding to the endogenous UVR8 and YFP-UVR8 whereas hybridization with anti-ACTIN

View Article Online
DOI: 10.1039/C8PP00492G

antibody was performed to check the amount of protein present in the lanes. Signals corresponding to the UVR8 and GFP-UVR8 bands were quantified, normalized to the corresponding ACTIN signal and compared to the endogenous UVR8 level in the Col background (100%). Supplementary Fig. 9. presents a repetition of the experiment.

Fig. 8 Flavonoid staining of the upper part of the hypocotyl. 2-day-old *uvr8-6* mutant seedlings, expressing the indicated transgenes were placed in white light supplemented with 1 μmol m^{-2} s^{-1} 311 nm adaxial UV-B (UV-B) or kept under a UV-B blocking cut-off filter of 385 nm (Control) for 3 days. Columbia (Col-0) and *uvr8-6* seedlings were also analysed. Samples were mounted and incubated in DPBA solution for 5 minutes before visualization using CLSM. Flavonol-DPBA complexes appear as green colour, whereas expression of YFP-UVR8 are shown as green signal using YFP-specific imaging settings of the microscope in separate images (YFP-UVR8). All images were taken with focal plane set on the vasculature. Scale bar indicates 100 μm.

View Article Online
DOI: 10.1039/C8PP00492G

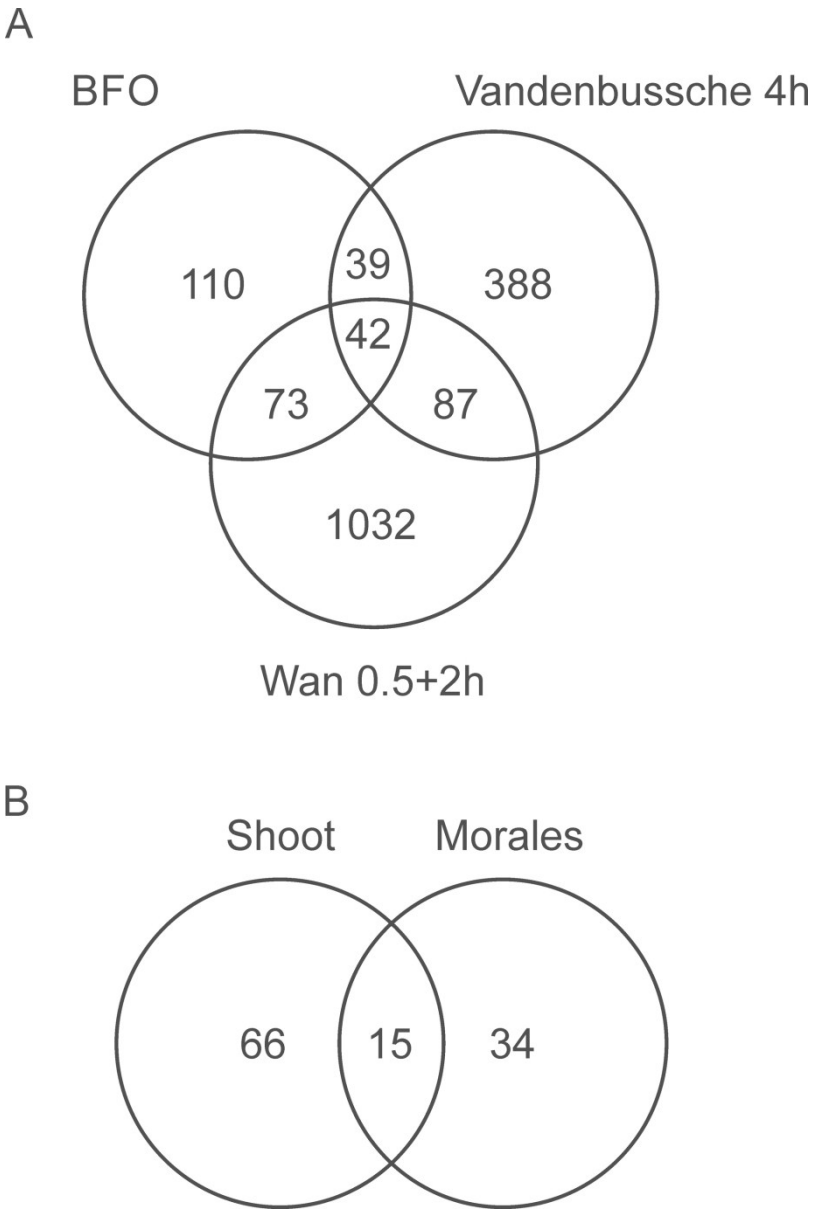

Fig. 1. Comparison of UV-B up-regulated genes throughout different datasets. (A) Venn diagram of UV-B up-regulated genes selected from the Brown & Jenkins, 2008; Favory et al, 2009; Oravecz et al, 2006 datasets (BFO) [4, 28, 52] as well as those from developing leaves (Vandenbussche et al, 2018 [53]) and roots (Wan et al, 2018 [54]). (B) Venn diagram comparing UV-B up-regulated genes in the shoot in controlled conditions (Shoot) with the UV-B up-regulated genes from the field experiment of Morales et al, 2013[57].

82x123mm (600 x 600 DPI)

View Article Online
DOI: 10.1039/C8PP00492G

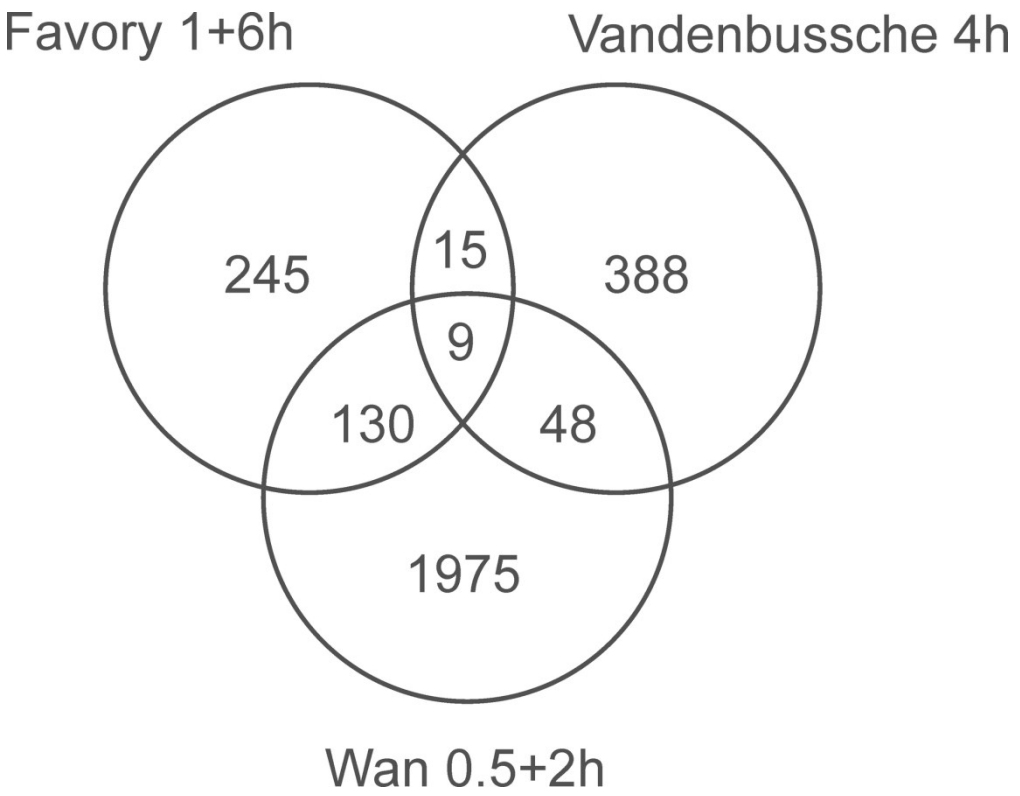

Fig. 2. Comparison of UV-B down-regulated genes throughout different datasets. Venn diagram of UV-B down-regulated genes selected from the Favory et al, 2009 dataset4, as well as those from developing leaves (Vandenbussche et al, 2018 [53]) and roots (Wan et al, 2018 [54]) datasets.

82x64mm (600 x 600 DPI)

View Article Online
DOI: 10.1039/C8PP00492G

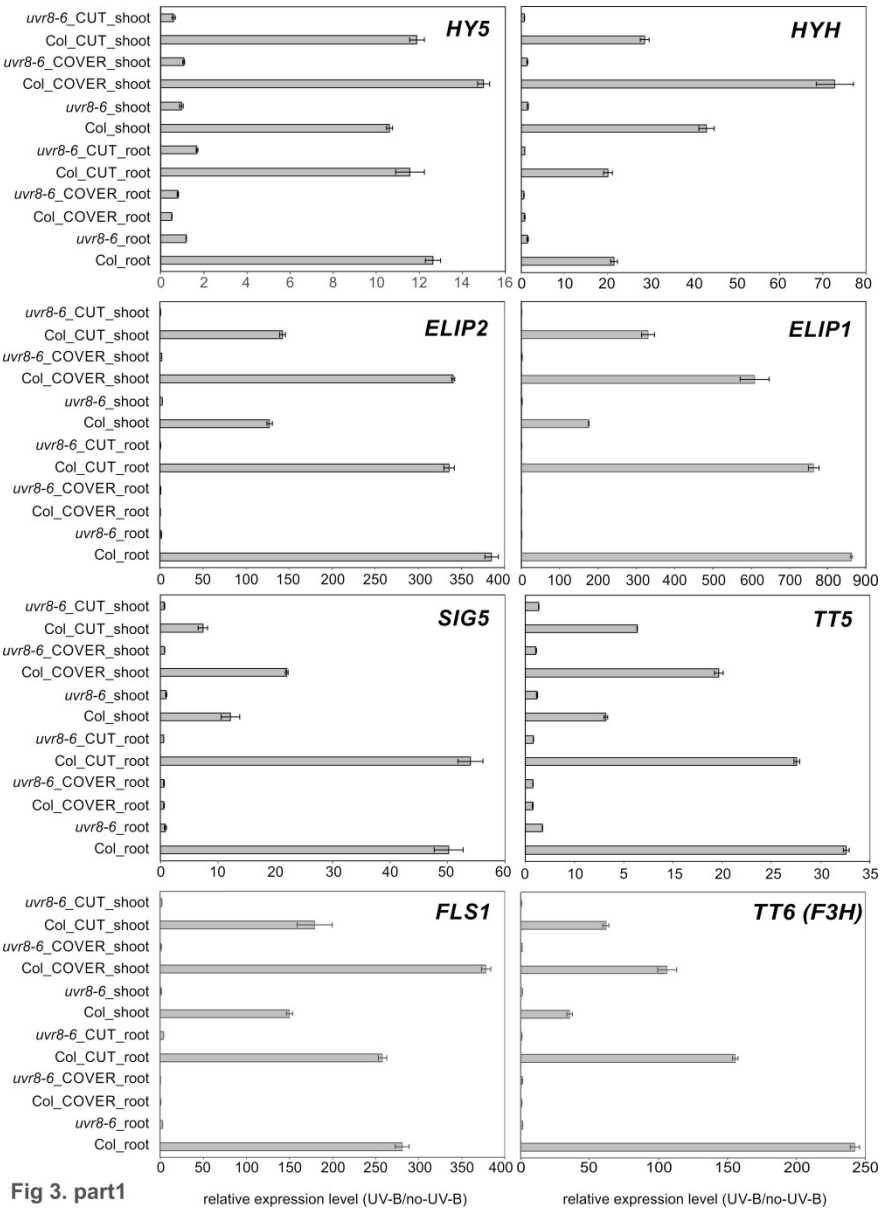

Fig. 3. part1

Fig. 3. Reporters of transcriptional changes in different plant organs. Columbia wild type and uvr8-6 plants were grown on vertical plates for 11 days and were irradiated with white light supplemented with UV-B or not supplemented for 2 h. Roots and shoots of the plants were collected separately. Samples from plants with roots covered during (COVER) or from plants with roots and shoots separated before the UV-B treatment (CUT) were also collected and analysed by qRT-PCR after total RNA extraction. The signals were normalized to the corresponding TUBULIN signal and relative values were determined (UV-B treated/non-treated plants). Error bars indicate standard error (n=3).

170x234mm (600 x 600 DPI)

View Article Online
DOI: 10.1039/C8PP00492G

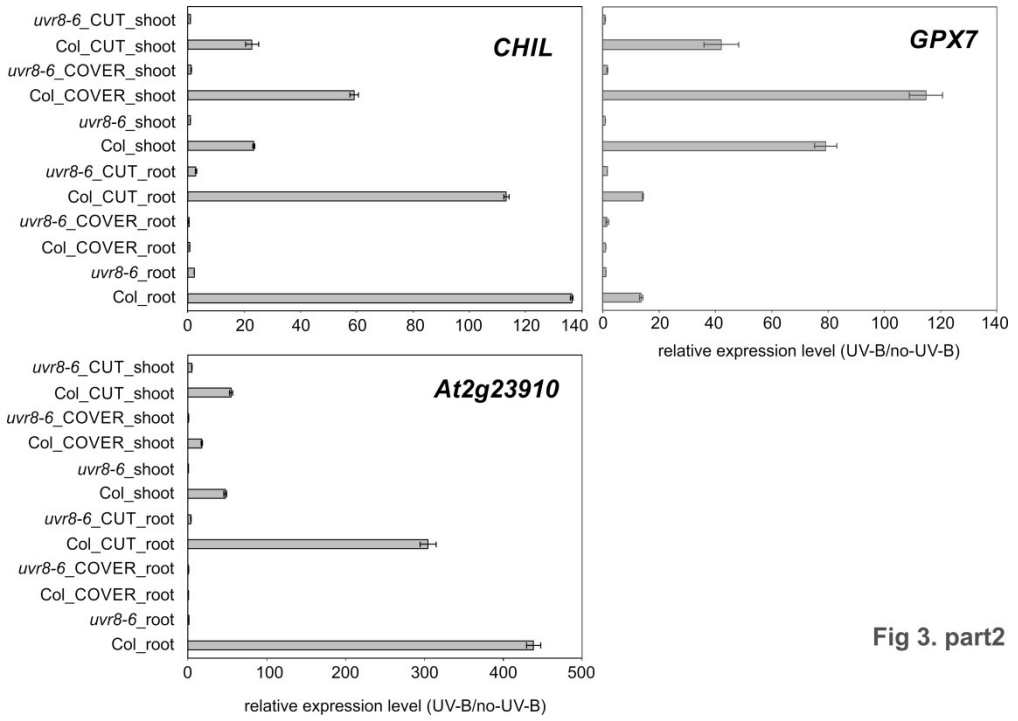

Fig 3. part2

Fig. 3. Reporters of transcriptional changes in different plant organs. Columbia wild type and uvr8-6 plants were grown on vertical plates for 11 days and were irradiated with white light supplemented with UV-B or not supplemented for 2 h. Roots and shoots of the plants were collected separately. Samples from plants with roots covered during (COVER) or from plants with roots and shoots separated before the UV-B treatment (CUT) were also collected and analysed by qRT-PCR after total RNA extraction. The signals were normalized to the corresponding TUBULIN signal and relative values were determined (UV-B treated/non-treated plants). Error bars indicate standard error (n=3).

170x121mm (600 x 600 DPI)

View Article Online
DOI: 10.1039/C8PP00492G

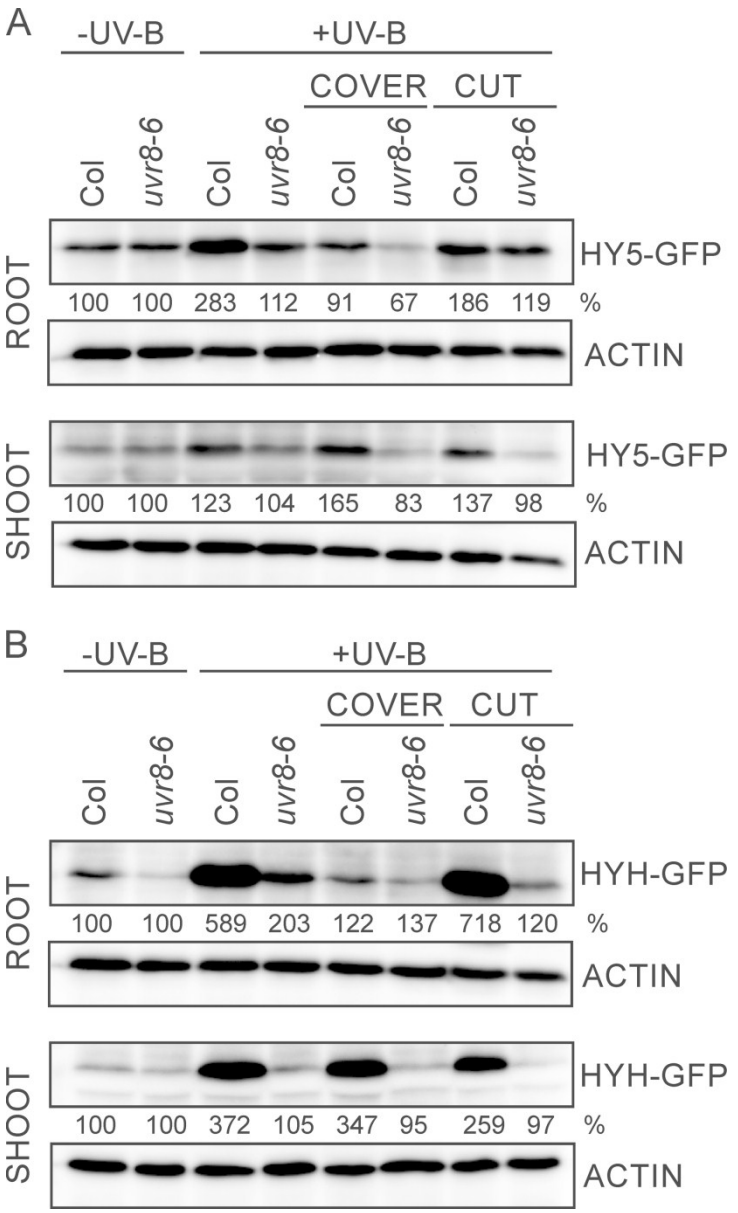

Fig. 4. Accumulation of HY5-GFP and HYH-GFP in different organs of Arabidopsis seedlings under UV-B irradiation. Columbia wild type and uvr8-6 plants expressing pHY5:HY5-GFP (panel A) or pHYH:HYH-GFP (panel B) were grown on vertical plates for 10 days and were irradiated with white light supplemented with UV-B (+UV-B) or not supplemented (-UV-B) for 20h. Roots or shoots (aerial parts) of the plants were collected separately. Samples from plants with roots covered during (COVER) or from plants with roots and shoots separated before the UV-B treatment (CUT) were also collected. The protein extracts were tested with western blot analysis using anti-GFP antibody to visualize bands corresponding to HY5-GFP (panel A) and HYH-GFP (panel B) whereas hybridization with anti-ACTIN antibody was performed to check the amount of protein present in the lanes. Signals corresponding to the HY5-GFP and HYH-GFP bands were quantified, normalized to the corresponding ACTIN signal. The -UV-B samples in both organs and both genotypes were set to 100%.

80x133mm (600 x 600 DPI)

View Article Online
DOI: 10.1039/C8PP00492G

View Article Online
DOI: 10.1039/C8PP00492G

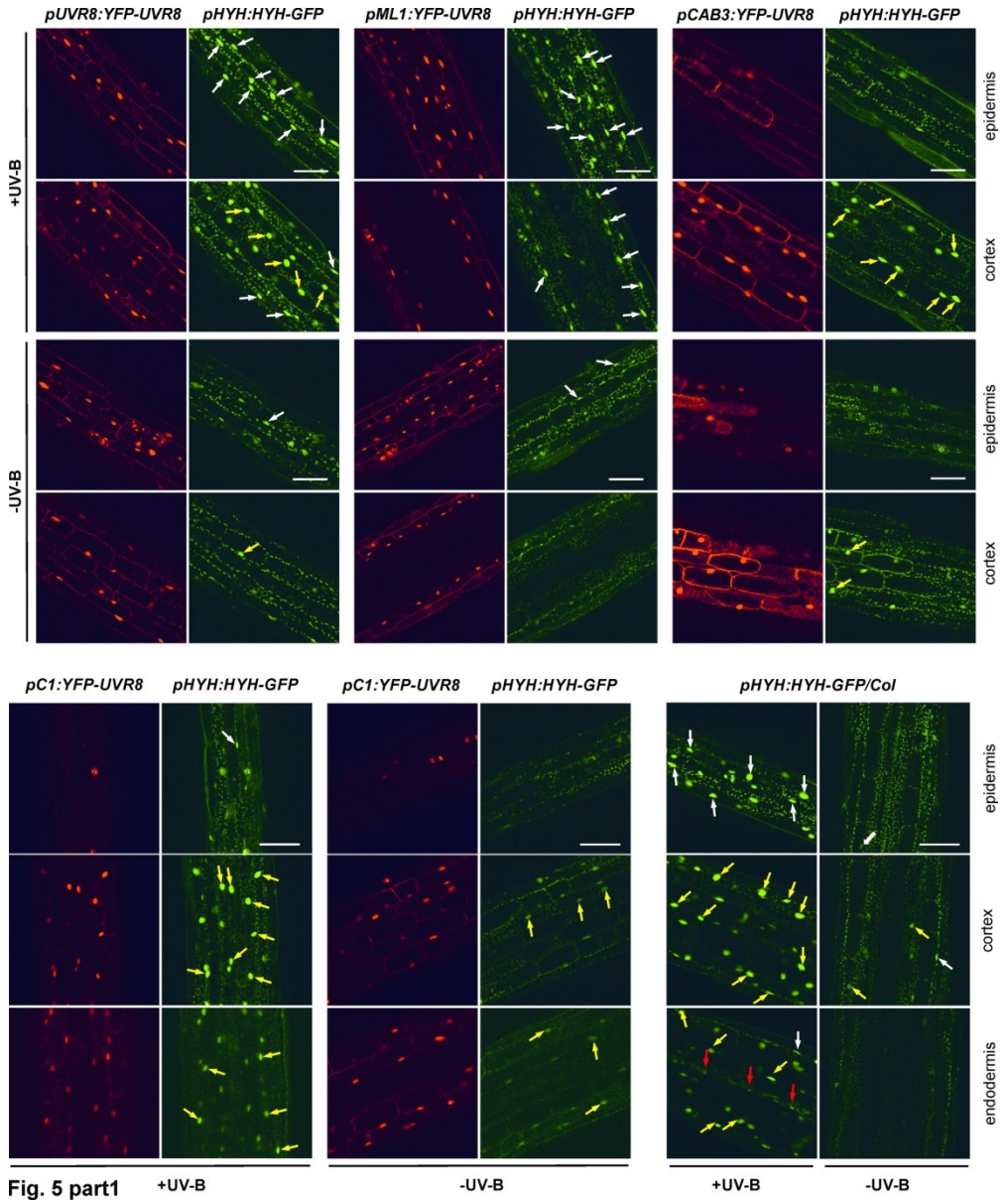

Fig. 5 part1

170x205mm (300 x 300 DPI)

View Article Online
DOI: 10.1039/C8PP00492G

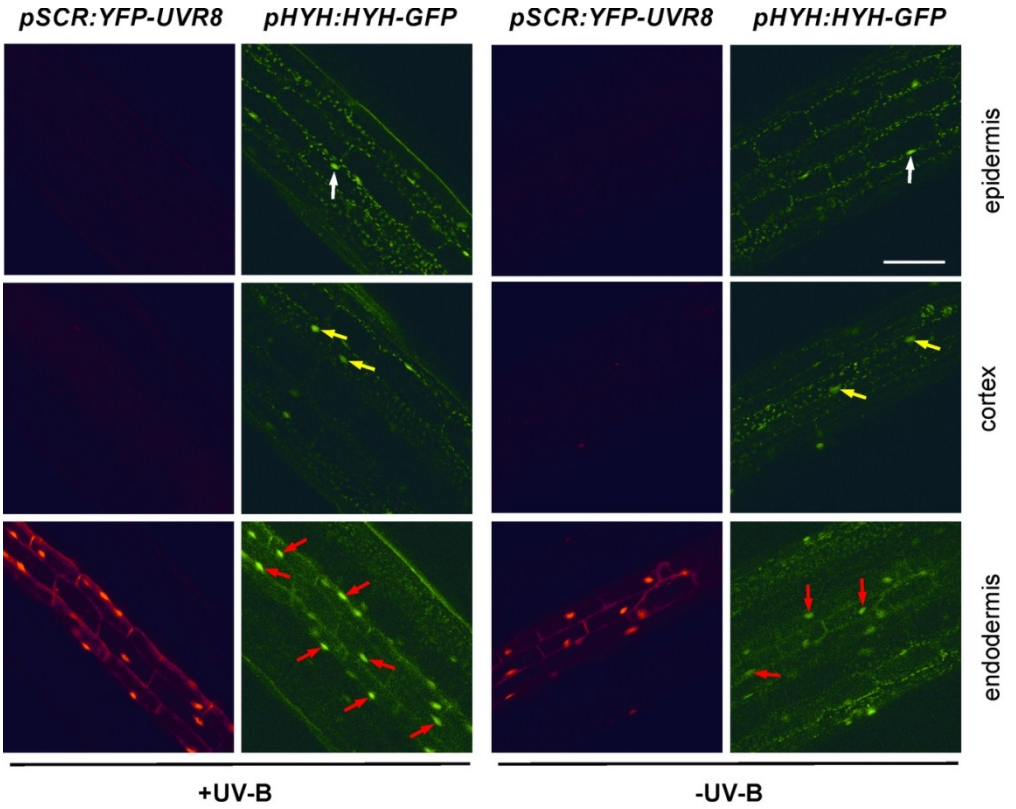

Fig. 5 part2

Fig. 5. UV-B induction of pHYH:HYH-GFP in the hypocotyl cells of transgenic lines expressing YFP-UVR8 in different tissues. pHYH:HYH-GFP was introduced into Columbia (Col) wild type and into transgenic uvr8-6 lines expressing pUVR8:YFP-UVR8, pML1:YFP-UVR8, pCAB3:YFP-UVR8, pC1:YFP-UVR8 or pSCR:YFP-UVR8. Localization of the HYH-GFP (green colour) and the YFP-UVR8 (red colour) fusion proteins were monitored by CLSM. The focal planes were set on the epidermis, cortex or endodermis cells of the hypocotyl of 6-day-old seedlings irradiated with constant WL supplemented with UV-B (+UV-B) or not supplemented (-UV-B) for 20 h. Identical microscope settings were used to allow determination of the difference between the visual signals of the +UV-B and –UV-B image pairs. White, yellow and red arrows indicate the positions of selected nuclei containing HYH-GFP signal in the epidermis, cortex and endodermis, respectively. Scale bars indicate 100 μm.

114x96mm (300 x 300 DPI)

View Article Online
DOI: 10.1039/C8PP00492G

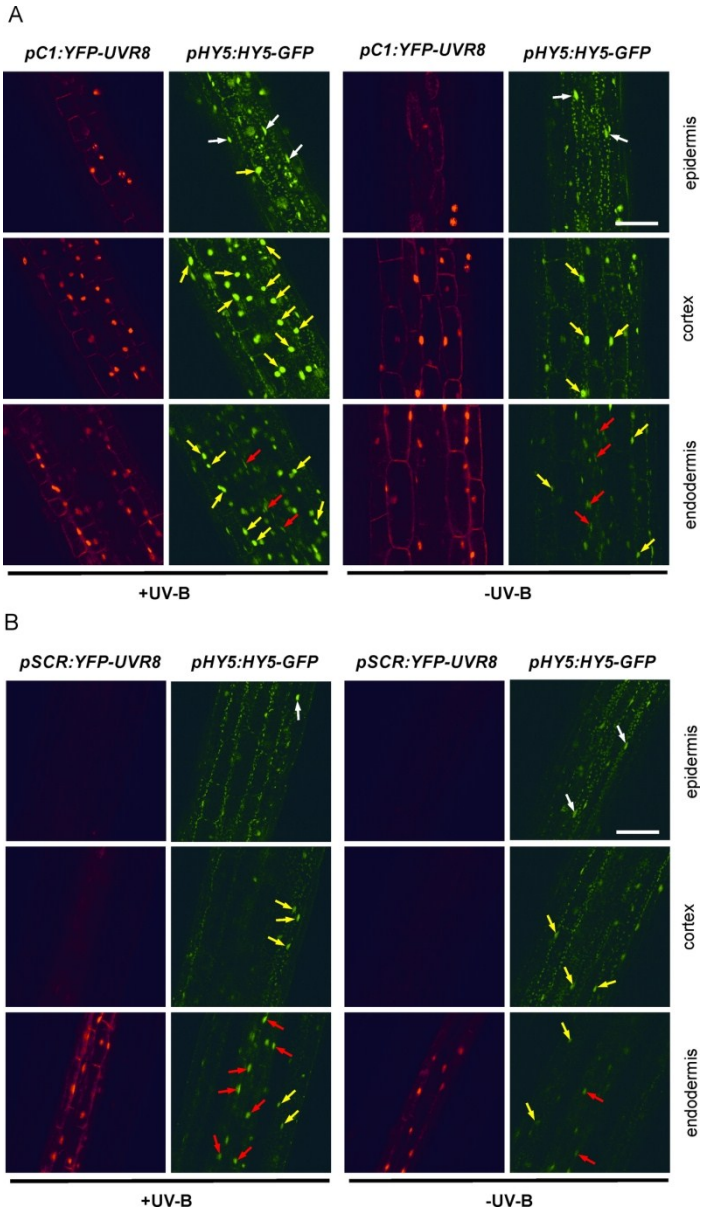

Fig. 6. UV-B induced accumulation of HY5-GFP in the hypocotyl cells of transgenic lines expressing YFP-UVR8 in different tissues. pHY5:HY5-GFP was introduced into transgenic uvr8-6 lines expressing pC1:YFP-UVR8 (panel A) or pSCR:YFP-UVR8 (panel B). Localization of the HY5-GFP (green colour) and the YFP-UVR8 (red colour) fusion proteins were monitored by CLSM. The focal planes were set on the epidermis, cortex and endodermis cells of the hypocotyl of 6-day-old seedlings irradiated with constant WL supplemented with UV-B (+UV-B) or not supplemented (-UV-B) for 20 h. Identical microscope settings were used to allow determination of the difference between the visual signals of the +UV-B and –UV-B image pairs. White, yellow and red arrows indicate the positions of selected nuclei containing HYH-GFP signal in the epidermis, cortex and endodermis, respectively. Scale bars indicate 100 μm.

114x197mm (300 x 300 DPI)

View Article Online
DOI: 10.1039/C8PP00492G

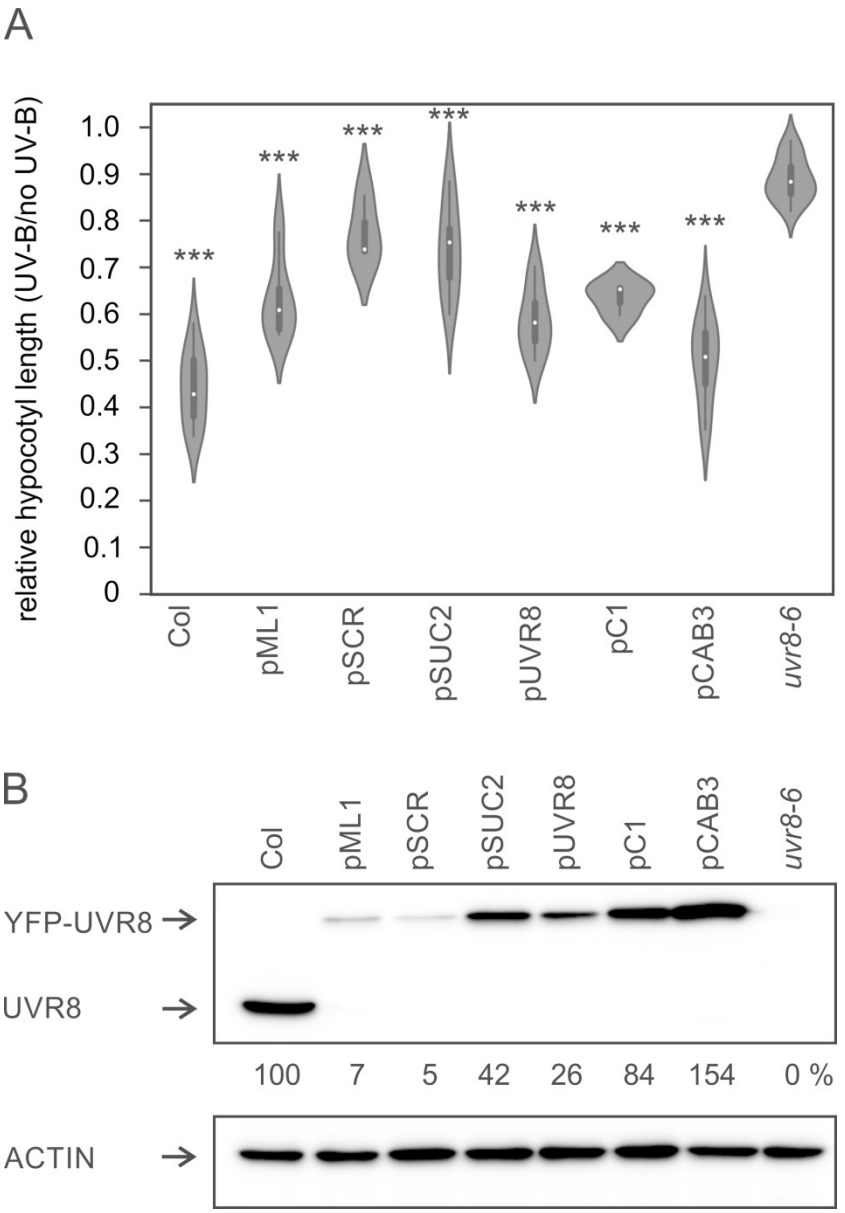

Fig. 7. Expression of YFP-UVR8 in different tissues contributes differently to hypocotyl elongation inhibition. A Seedlings were grown under constant white light supplemented with or without 1.5 µmol m-2 s-1 UV-B for 7 days, their hypocotyl length was measured and the relative hypocotyl length values were calculated and spotted. Together with the wild type Columbia (Col) uvr8-6 mutant and uvr8-6 mutant expressing proUVR8:YFP-UVR8 (pUVR8). proML1:YFP-UVR8 (pML1), proCAB3:YFP-UVR8 (pCAB3), proSUC2:YFP-UVR8 (pSUC2), proC1:YFP-UVR8 (pC1), proSCR:YFP-UVR8 (pSCR) transgenes were included in the assay. Each measurement was repeated at least 3 times. Asterisks mark lines that display significant differences as compared with the uvr8-6 mutant line calculated by the Student's t-test (significance: ***P< 0.005). B. Seedlings were grown under constant WL supplemented with UV for 7 days before total protein extraction. The protein extracts were tested with western blot analysis using anti-UVR8 antibody to visualize bands corresponding to the endogenous UVR8 and YFP-UVR8 whereas hybridization with anti-ACTIN antibody was performed to check the amount of protein present in the lanes. Signals corresponding to the UVR8 and GFP-UVR8 bands were quantified, normalized to the corresponding ACTIN signal and compared to the endogenous UVR8 level in the Col background (100%). Supplementary Fig. 9 presents a repetition of the

View Article Online
DOI: 10.1039/C8PP00492G

experiment.

80x115mm (600 x 600 DPI)

View Article Online
DOI: 10.1039/C8PP00492G

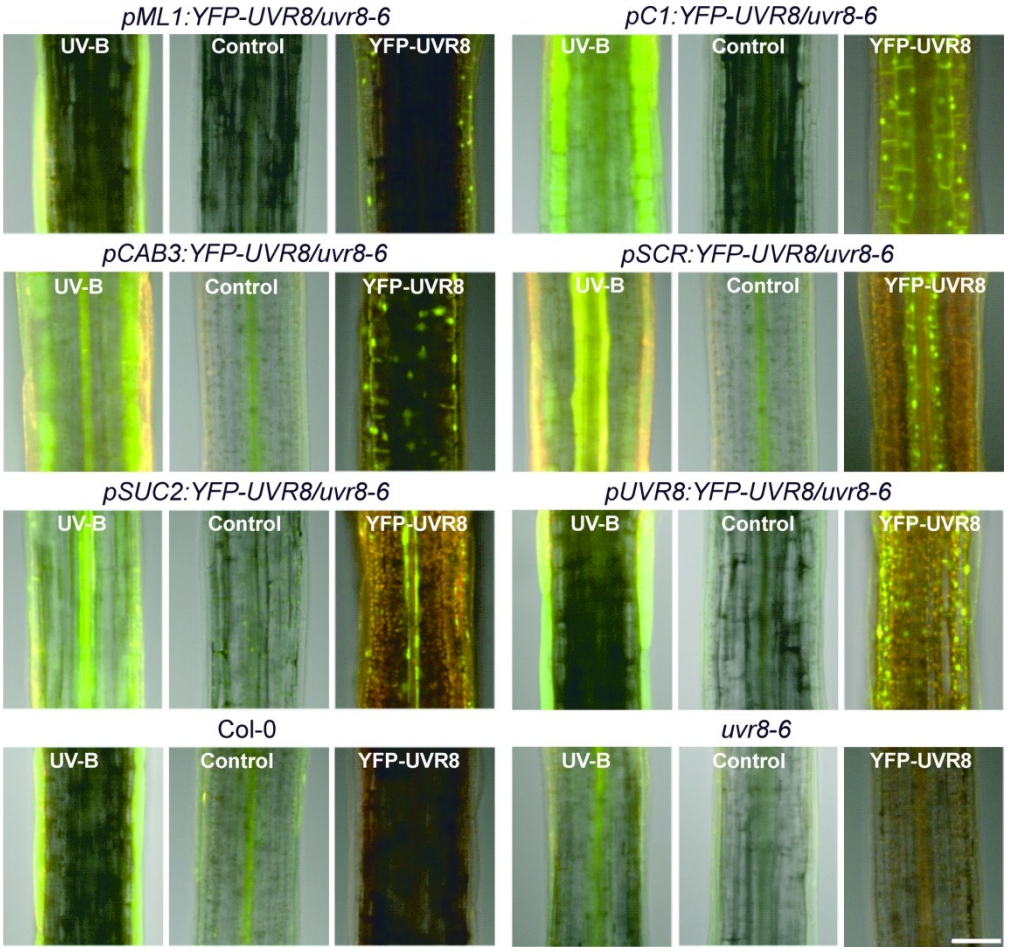

Fig. 8 Flavonoid staining of the upper part of the hypocotyl. 2-day-old uvr8-6 mutant seedlings, expressing the indicated transgenes were grown in white light exposed to 1 µmol m-2 s-1 311 nm adaxial UV-B (UV-B) or kept under a UV-B blocking cut-off filter of 385 nm (Control) for 3 days. Columbia (Col-0) and uvr8-6 seedlings were also analysed. Samples were mounted and incubated in DPBA solution for 5 minutes before visualization using CLSM. Flavonol-DPBA complexes appear as green colour, whereas expression of YFP-UVR8 are shown as green signal using YFP-specific imaging settings of the microscope in separate images (YFP-UVR8). All images were taken with focal plane set on the vasculature. Scale bar indicates 100 µm.

170x159mm (300 x 300 DPI)

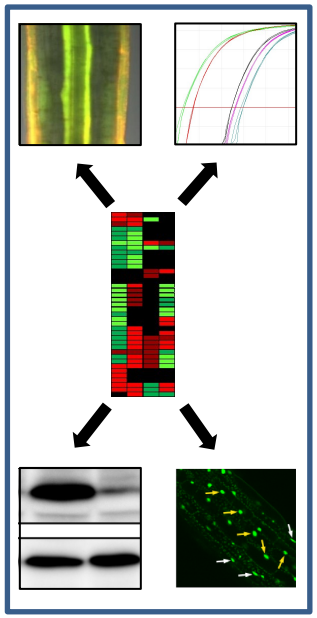

Text forthe graphical abstract:
We demonstrate the identification and application of molecular reporters and phenotypic traits to monitor the dynamics of the still largely unknown UVR8-dependent signalling pathways.